

LIDAR REMOTE SENSING DATA COLLECTION: Columbia River Survey Final Delivery

September 22nd, 2010

Submitted to:

Jacob MacDonald
U.S. Army Corps of Engineers
Portland District
P.O. Box 2946
Portland, OR 97208



Submitted by:

Watershed Sciences
517 SW 2nd Street, Suite 400
Corvallis, OR 97333

529 SW 3rd Ave. Suite 300
Portland, OR 97204



LIDAR REMOTE SENSING DATA COLLECTION: COLUMBIA RIVER SURVEY FINAL DELIVERY

TABLE OF CONTENTS

1. Overview.....	1
2. Acquisition.....	3
2.1 Airborne Survey - Instrumentation and Methods.....	3
2.2 Ground Survey - Instrumentation and Methods	4
2.2.1 Survey Control	4
2.2.2 RTK Survey	9
3. LiDAR Data Processing	11
3.1 Applications and Work Flow Overview	11
3.2 Aircraft Kinematic GPS and IMU Data	12
3.3 Laser Point Processing	12
4. LiDAR Accuracy Assessment.....	13
4.1 Laser Noise and Relative Accuracy.....	13
4.2 Absolute Accuracy.....	14
5. Study Area Results.....	15
5.1 Data Summary.....	15
5.2 Data Density/Resolution.....	16
5.3 Relative Accuracy Calibration Results.....	47
5.4 Absolute Accuracy.....	49
6. Breakline Enforced Terrain Model.....	51
7. Projection/Datum and Units	52
8. Deliverables	52
9. Selected Images	53
10. Glossary.....	66
11. Citations	67
Appendix A.....	68
Appendix B.....	70

1. Overview

Watershed Sciences, Inc. (WS) collected Light Detection and Ranging (LiDAR) data of the Columbia River in Oregon, Washington, Idaho, and Montana. The requested AOI area for delivery 12 was 23,314 acres. The area was expanded to include a 100m buffer to ensure complete coverage and adequate point densities around survey area boundaries, resulting in 33,045 acres of delivered data. LiDAR data for Delivery 12 was collected on November 21st, 2009 and between June 29th and July 1st, 2010 (**Figure 1**). This area includes the Snake River from north of the confluence with the Grande Ronde River to the Brownlee Dam and Reservoir. This report contains maps and information specific to Delivery 12, but has been appended to the previous delivered reports to generate a cumulative data summary for UTM Zone 10 and 11. This report completes the delivery of the Columbia River project data and contains the final cumulative accuracy and density data for UTM 10 and UTM 11.

Watershed Sciences performed this work under US Army Corp of Engineers Contract No. WS9127N-09-D-0009 as a sub consultant to and in partnership with:

- 1. David Smith and Associates, Inc. , 1734 SE Tacoma St, Portland, OR 97202
- 2. AECOM Environment, 9521 Willows Road NE, Redmond, WA 98052

Figure 1. Columbia River survey delivery status overview.



Table 1. Columbia River, UTM Zone 10 and 11 LiDAR deliveries to date.

UTM 10 Delivery	Date	Total Acres Flown	AOI Acres
1	April 15, 2010	129,000	125,409
2	May 13, 2010	191,071	181,694
4	June 8, 2010	324,600	314,797
8	July 22, 2010	104,774	94,054
UTM 11 Delivery	Date	Total Acres Flown	AOI Acres
1	April 15, 2010	206,500	187,764
3	May 20, 2010	115,200	102,837
5	June 17, 2010	52,785	44,273
6	June 23, 2010	99,741	89,405
6b	July 1, 2010	67,729	60,369
7	July 16, 2010	187,130	170,290
8	July 22, 2010	55,374	51,985
9	July 29, 2010	115,148	103,574
10	August 11, 2010	73,376	61,890
11	September 3, 2010	215,077	206,986
12	September 22, 2010	33,045	23,314
Project Total		1,970,550	1,818,641

2. Acquisition

2.1 Airborne Survey - Instrumentation and Methods

The LiDAR survey uses Leica ALS50 Phase II and ALS60 laser systems. For the Columbia River survey sites, the sensor scan angle was $\pm 14^\circ$ from nadir¹ with a pulse rate designed to yield an average native density (number of pulses emitted by the laser system) of ≥ 8 points per square meter over terrestrial surfaces. It is not uncommon for some types of surfaces (e.g. dense vegetation or water) to return fewer pulses than the laser originally emitted. These discrepancies between ‘native’ and ‘delivered’ density will vary depending on terrain, land cover and the prevalence of water bodies.



The Cessna Caravan is a stable platform, ideal for flying slow and low for high density projects. The Leica ALS60 sensor head installed in the Caravan is shown on the left.

All areas were surveyed with an opposing flight line side-lap of $\geq 50\%$ ($\geq 100\%$ overlap) to reduce laser shadowing and increase surface laser painting. The Leica laser systems allow up to four range measurements (returns) per pulse, and all discernable laser returns were processed for the output dataset.

To accurately solve for laser point position (geographic coordinates x, y, z), the positional coordinates of the airborne sensor and the attitude of the aircraft were recorded continuously throughout the LiDAR data collection mission. Aircraft position was measured twice per second (2 Hz) by an onboard differential GPS unit. Aircraft attitude was measured 200 times per second (200 Hz) as pitch, roll and yaw (heading) from an onboard inertial measurement unit (IMU). To allow for post-processing correction and calibration, aircraft/sensor position and attitude data are indexed by GPS time.

¹ Nadir refers to the perpendicular vector to the ground directly below the aircraft. Nadir is commonly used to measure the angle from the vector and is referred to a “degrees from nadir”.

2.2 Ground Survey - Instrumentation and Methods

The following ground survey data were collected to enable the geo-spatial correction of the aircraft positional coordinate data collected throughout the flight, and to allow for quality assurance checks on final LiDAR data products.



2.2.1 Survey Control

Simultaneous with the airborne data collection mission, multiple static (1 Hz recording frequency) ground surveys were conducted over monuments with known coordinates (**Table 2**). Survey control monuments were occupied by a Trimble GPS base station for an initial period of at least eight hours. All monuments were occupied during a subsequent second session with an observation period of at least four hours. Additional occupations were conducted as necessary. GPS measurements were made with dual frequency L1-L2 receivers with carrier-phase correction.

David Evans and Associates (DEA), Portland, OR provided PLS (Professional Licensed Surveyor) supervision and oversight for the entire Columbia River project. DEA processed all static GPS occupations and provided Watershed Sciences with certified coordinates for all LiDAR mapping control. In addition, DEA published a mapping control through the OPUS online database publication tool located on the NGS website. All monuments used by Watershed Sciences were published and made publically available by DEA on the OPUS online datasheet website (Please see "Columbia River Treaty OPUS DB Data Sheets" DVD for DEA's full report).

Watershed Sciences established monuments using aluminum survey caps provided by the Army Corps of Engineers. Monuments were placed using 5/8" by 30" rebar covered with a 2" top aluminum cap stamped "U.S. Army C. of E. Portland Dist.". In addition, monuments were stamped in the field with the year and monument ID number.

As an initial check, the NGS on-line positioning user service (OPUS), was used to generate a corrected position for all base station observations. OPUS provides a measurement solution based on three surrounding continuously operating reference stations (CORS). OPUS output includes a solution report with positional accuracy confidence intervals for adjusted coordinates and elevations. The solution report is one component in assessing the quality of the OPUS GPS measurement solutions. Statistical checks of GPS base station positions and repeat control observations include the OPUS solution extended output report. In addition, the standard deviation, kurtosis, and skew of the measurement distribution for each base station occupation were compared. Longitude, latitude, and elevation distributions were separated, and graphic distributions of the positions were plotted for consistency.

Indexed by time, these GPS data are used to correct the continuous onboard measurements of aircraft position recorded throughout the mission. Control monuments were located within 13 nautical miles of the survey area(s).

Table 2. DEA Certified Survey Control coordinates for Columbia River, UTM Zones 10 and 11 (DEA, 2010).

Base Station ID	Datum: NAD83 (CORS96)		GRS80
	Latitude	Longitude	Ellipsoid Z (m)
1001-02	48 23 56.98482	-115 34 50.21483	616.831
1001-03	48 26 14.03972	-115 51 23.02348	629.994
1001-04	48 32 51.20358	-115 57 51.74806	548.385
1001-05	48 48 13.76901	-116 19 54.78221	668.822
1001-06	48 44 31.95802	-116 16 27.48836	696.109
1001-07	48 54 15.05346	-116 23 33.02882	521.523
1001-08	46 30 08.41845	-116 25 47.09675	418.636
1001-09	46 29 22.56717	-116 36 33.78201	660.133
1001-10	46 26 48.57603	-116 49 22.85153	242.283
1001-11	46 25 37.24185	-116 59 37.84845	209.654
1001-12	46 25 28.18217	-117 02 53.46337	217.828
1001-14	46 31 44.00816	-117 17 42.94603	806.850
1001-15	46 09 54.03858	-117 05 33.99519	976.572
1001-16	46 17 49.31959	-117 02 40.71052	630.840
1001-17	46 37 03.17427	-117 24 34.40297	712.061
1001-18	46 33 18.67588	-118 02 38.51875	431.742
1001-19	46 33 41.76244	-117 53 55.49244	401.264
1001-22	45 56 4.36406	-116 34 44.52313	1465.413
1001-23	45 48 37.14700	-116 27 47.99809	1315.761
1001-25	46 15 24.33299	-119 06 44.28022	99.580
1001-26	46 04 58.38585	-118 54 08.97171	95.397
1001-27	46 32 46.94111	-118 32 25.89962	226.994
1001-29	45 56 24.58774	-119 18 39.87547	74.982
1001-30	45 53 42.93963	-119 30 34.66550	68.346
1001-31	46 19 13.63661	-118 45 33.52351	144.348
1001-32	46 26 46.23824	-119 14 59.85289	171.387
1001-33	46 35 03.15570	-119 17 48.43777	264.490
1001-34	46 42 39.57396	-119 57 04.04702	132.138
1001-35	46 54 34.61756	-119 56 52.68161	245.487
1001-36	46 38 32.50510	-119 44 38.56540	107.820
1001-37	47 13 44.45738	-120 0 43.49207	257.131
1001-38	47 31 01.69423	-120 17 43.85407	205.566
1001-39	47 43 16.43454	-120 12 05.54248	279.646
1001-40	47 39 26.74447	-120 12 51.23753	201.909
1001-41	47 52 34.16625	-119 55 30.35960	359.683

Base Station ID	Datum: NAD83 (CORS96)		GRS80
	Latitude	Longitude	Ellipsoid Z (m)
1001-42	48 39 42.07553	-117 23 30.60187	622.832
1001-43	48 51 35.80852	-117 22 12.13785	626.785
1001-44	48 20 17.00710	-117 17 38.10574	609.766
1001-45	48 04 42.09424	-115 58 11.36504	684.158
1001-46	47 53 57.17442	-115 40 38.25177	749.758
1001-47	47 42 25.79030	-115 26 45.85658	764.153
1001-48	47 31 31.28040	-115 0 36.84563	730.067
1001-49	46 09 55.00289	-123 08 46.34550	-15.171
1001-50	45 40 13.04473	-122 45 28.31957	-14.798
1001-51	45 32 52.95214	-122 24 43.61919	-13.122
1001-52	45 41 51.83136	-122 44 01.68085	-14.212
1001-53	45 35 59.70787	-122 37 05.21497	-9.882
1001-54	45 27 24.11550	-122 33 34.92185	180.288
1001-55	45 53 58.62988	-122 47 51.37726	-13.396
1001-56	45 51 15.81779	-122 42 09.46590	52.603
1001-57	46 02 26.42971	-122 52 01.38200	-14.220
1001-58	46 06 32.94920	-122 53 01.76745	-13.834
1001-59	47 54 08.17176	-118 20 03.21717	391.203
1001-60	48 11 09.36642	-117 01 49.51670	610.614
1001-62	48 07 48.72502	-119 18 57.73566	348.902
1001-63	48 01 58.81548	-118 57 40.44020	313.960
1001-64	48 07 07.96832	-118 13 10.22406	462.187
1001-65	47 55 43.85009	-118 41 20.44432	376.281
1001-66	47 52 22.12504	-118 19 29.21408	543.652
1001-67	48 01 32.65643	-119 34 09.57665	313.446
1001-68	45 42 41.45723	-121 46 39.21045	13.710
1001-69	45 36 9.27614	-122 2 37.57830	0.204
1001-70	45 54 49.89396	-122 48 12.52957	-13.482
1001-71	46 10 44.41058	-123 22 37.98798	-16.494
1001-72	46 14 15.72282	-123 23 47.41730	-17.845
1001-73	46 21 04.74607	-123 36 24.40429	-16.407
1001-74	46 21 11.60474	-123 48 45.17118	-10.861
1001-75	46 10 23.59054	-123 49 53.71402	-18.456
1001-76	47 52 21.92656	-118 19 29.68485	543.446
1001-77	48 05 40.67814	-118 13 22.57872	444.409
1001-78	48 15 21.98771	-118 08 01.18819	379.954

Base Station ID	Datum: NAD83 (CORS96)		GRS80
	Latitude	Longitude	Ellipsoid Z (m)
1001-79	48 26 26.39581	-118 10 13.95487	521.192
1001-80	45 42 49.27090	-121 30 39.83749	6.517
1001-81	45 40 29.62695	-121 15 50.33345	11.637
1001-82	45 38 19.36273	-120 58 01.24913	207.447
1001-83	45 43 47.54805	-120 39 04.19716	75.569
1001-84	45 42 04.13225	-120 20 40.20502	150.893
1001-85	45 47 05.76648	-120 02 18.05975	109.677
1001-86	45 50 33.55651	-119 42 34.81642	65.288
1001-87	46 11 28.87024	-123 45 29.15267	-1.992
1001-88	46 12 49.68406	-123 32 29.63950	-21.069
1001-89	46 12 49.74473	-123 32 29.55793	-21.065
1001-90	46 09 11.71519	-123 52 41.61197	-19.966
1001-91	46 11 48.84319	-118 58 46.57016	99.304
1001-92	48 11 13.44329	-116 26 13.31352	614.124
1001-93	48 07 22.89093	-116 09 43.76442	617.352
1001-94	48 10 32.72793	-116 13 56.37429	614.029
1001-95	45 23 55.10893	-116 43 39.37875	1996.293
1001-96	48 19 22.29241	-116 26 54.84908	626.669
1001-97	48 13 57.90901	-116 31 44.49034	618.705
1001-98	48 51 09.21908	-117 53 28.28571	466.493
1001-99	48 54 44.63988	-117 47 25.87213	396.158
1001-100	48 34 12.52863	-118 06 49.31297	376.733
1001-101	48 43 02.83908	-118 01 34.25317	392.519
1001-103	48 19 50.72828	-114 11 47.13329	913.855
1001-104	48 18 32.50920	-114 13 58.76651	887.556
1001-105	48 2 36.45821	-116 67 55.66440	684.057
1001-106	48 43 14.07373	-116 18 37.83016	681.969
1001-107	47 49 55.98524	-115 35 13.49428	706.003
1001-108	47 26 26.50061	-114 52 29.24524	736.687
1001-109	47 34 38.93062	-115 18 16.78201	727.692
1001-110	47 20 27.83571	-114 37 54.76413	763.841
1001-111	47 18 47.09352	-114 21 25.31047	753.416
1001-112	47 29 18.70339	-114 20 30.58228	825.889
1001-113	48 04 52.09014	-114 05 57.68806	888.638
1001-114	47 52 02.68632	-114 16 28.44232	870.056
1001-120	45 26 6.14033	-116 40 1.50614	2085.747

Base Station ID	Datum: NAD83 (CORS96)		GRS80
	Latitude	Longitude	Ellipsoid Z (m)
1001-121	47 41 34.65105	-114 11 05.77338	879.665
1001-122	47 41 34.16354	-114 11 06.37528	879.636
1001-123	48 07 27.25462	-114 11 31.97132	869.285
1001-124	48 07 15.01784	-114 14 25.37373	873.092
1001-125	48 23 40.92084	-115 33 37.77048	615.561
1001-126	45 11 34.19511	-116 45 48.09292	1857.514
1001-127	45 5 33.56314	-116 50 52.82256	1646.447
1001-129	46 2 8.92019	-116 50 43.21766	1545.937
1001-130	44 52 43.90824	-116 38 51.97408	1400.467
1001-131	44 53 49.01266	-116 41 7.76768	1498.534
86-19-305	46 11 52.54563	-122 54 46.81344	-6.618
AD9155	46 09 32.38751	-123 53 12.26752	-20.448
AD9552	46 18 21.26198	-119 18 36.67971	100.325
SD0651	46 13 31.35468	-124 00 30.58787	-14.296
SU0682	47 50 08.06221	-114 20 07.84551	881.843
DH8973	48 18 12.73636	-116 33 18.87333	631.363

2.2.2 RTK Survey

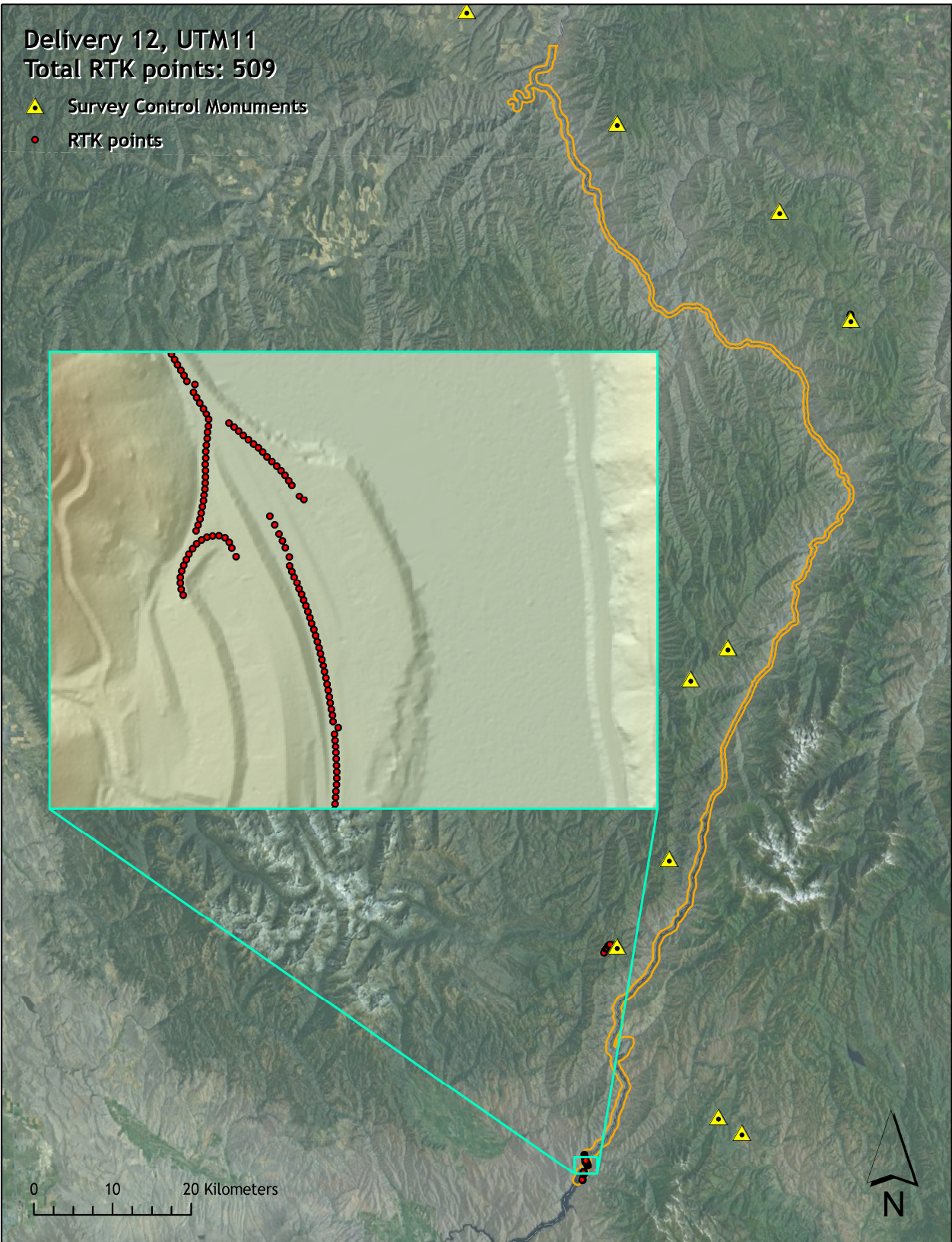
To enable assessment of LiDAR data accuracy, ground check points were collected using GPS based real-time kinematic (RTK) surveying. Instrumentation included multiple Trimble DGPS units (R8). RTK surveying allows for precise location measurements with an error (σ) of ≤ 1.5 cm (0.6 in).

For the RTK survey, the ground crew used a roving unit to receive radio-relayed corrected positional coordinates for all ground truth points from a GPS base station set up over certified survey control monuments. **Figure 2**, below, portrays the distribution of RTK points and base station locations used for the current delivery of Columbia River survey areas. RTK points were collected on hard surfaces that were easily distinguishable within the LiDAR dataset. Paved surfaces, including roads, paths, and parking lots, were the primary surface target. After all paved surfaces had been exhausted, hard packed gravel roads became the secondary target for RTK, followed by hard packed dirt roads. Hard surfaces are targeted in areas that are clearly visible (and likely to remain visible) from the sky during data acquisition.

In order to facilitate comparisons with LiDAR data, RTK measurements were not taken on highly reflective surfaces such as center line stripes or lane markings on roads. RTK points were taken no closer than one meter to any nearby terrain breaks such as road edges or drop offs to ensure an accurate comparison between RTK and LiDAR ground data. In addition, attempts were made to collect RTK points on locations that could be readily identified and occupied during subsequent field visits. RTK measurements were collected approximately 1-2 meters from one another to support measurement independence.

An RTK point acquisition period is five seconds long and includes three individual one-second measurements averaged together. The five second observation period ensures that an accurate RTK point was taken. RTK points were not taken during periods when PDOP was greater than three, when less than six satellites were visible, or when horizontal and vertical RMS values were greater than 0.03 m. An RMS value of 0.03 m indicates that an RTK measurement is within 0.03 m of its actual position 68% of the time. An RTK check point was also taken at the beginning and end of each RTK session as close to the base station location as possible to provide an on-the-spot vertical accuracy check.

Figure 2. RTK point and control monument locations used in Delivery 12, UTM 11.



3. LiDAR Data Processing

3.1 Applications and Work Flow Overview

1. Resolved kinematic corrections for aircraft position data using kinematic aircraft GPS and static ground GPS data.

Software: Waypoint GPS v.8.10, Trimble Geomatics Office v.1.62

2. Developed a smoothed best estimate of trajectory (SBET) file that blends post-processed aircraft position with attitude data. Sensor head position and attitude were calculated throughout the survey. The SBET data were used extensively for laser point processing.

Software: IPAS v.1.35

3. Calculated laser point position by associating SBET position to each laser point return time, scan angle, intensity, etc. Created raw laser point cloud data for the entire survey in *.las (ASPRS v. 1.2) format.

Software: ALS Post Processing Software v.2.69

4. Imported raw laser points into manageable blocks (less than 500 MB) to perform manual relative accuracy calibration and filter for pits/birds. Ground points were then classified for individual flight lines (to be used for relative accuracy testing and calibration).

Software: TerraScan v.10.009

5. Using ground classified points per each flight line, the relative accuracy was tested. Automated line-to-line calibrations were then performed for system attitude parameters (pitch, roll, heading), mirror flex (scale) and GPS/IMU drift. Calibrations were performed on ground classified points from paired flight lines. Every flight line was used for relative accuracy calibration.

Software: TerraMatch v.10.006

6. Position and attitude data were imported. Resulting data were classified as ground and non-ground points. Statistical absolute accuracy was assessed via direct comparisons of ground classified points to ground RTK survey data. Data were then converted to orthometric elevations (NAVD88) by applying a Geoid09 correction.

Software: TerraScan v.10.009, TerraModeler v.10.004

7. Bare Earth models were created as a triangulated surface with water and terrain breaklines enforced and exported as ArcInfo ASCII grids at a 1-meter pixel resolution. Highest Hit models were created for any class at 1-meter grid spacing and exported as ArcInfo ASCII grids.

Software: TerraScan v.10.009, ArcMap v. 9.3.1, TerraModeler v.10.004

3.2 Aircraft Kinematic GPS and IMU Data

LiDAR survey datasets were referenced to the 1 Hz static ground GPS data collected over pre-surveyed monuments with known coordinates. While surveying, the aircraft collected 2 Hz kinematic GPS data, and the onboard inertial measurement unit (IMU) collected 200 Hz aircraft attitude data. Waypoint GPS v.8.10 was used to process the kinematic corrections for the aircraft. The static and kinematic GPS data were then post-processed after the survey to obtain an accurate GPS solution and aircraft positions. IPAS v.1.35 was used to develop a trajectory file that includes corrected aircraft position and attitude information. The trajectory data for the entire flight survey session were incorporated into a final smoothed best estimated trajectory (SBET) file that contains accurate and continuous aircraft positions and attitudes.

3.3 Laser Point Processing

Laser point coordinates were computed using the IPAS and ALS Post Processor software suites based on independent data from the LiDAR system (pulse time, scan angle), and aircraft trajectory data (SBET). Laser point returns (first through fourth) were assigned an associated (x, y, z) coordinate along with unique intensity values (0-255). The data were output into large LAS v. 1.2 files; each point maintains the corresponding scan angle, return number (echo), intensity, and x, y, z (easting, northing, and elevation) information.

These initial laser point files were too large for subsequent processing. To facilitate laser point processing, bins (polygons) were created to divide the dataset into manageable sizes (< 500 MB). Flightlines and LiDAR data were then reviewed to ensure complete coverage of the survey area and positional accuracy of the laser points.

Laser point data were imported into processing bins in TerraScan, and manual calibration was performed to assess the system offsets for pitch, roll, heading and scale (mirror flex). Using a geometric relationship developed by Watershed Sciences, each of these offsets was resolved and corrected if necessary.

LiDAR points were then filtered for noise, pits (artificial low points) and birds (true birds as well as erroneously high points) by screening for absolute elevation limits, isolated points and height above ground. Each bin was then manually inspected for remaining pits and birds and spurious points were removed. In a bin containing approximately 7.5-9.0 million points, an average of 50-100 points are typically found to be artificially low or high. Common sources of non-terrestrial returns are clouds, birds, vapor, haze, decks, brush piles, etc.

Internal calibration was refined using TerraMatch. Points from overlapping lines were tested for internal consistency and final adjustments were made for system misalignments (i.e., pitch, roll, heading offsets and scale). Automated sensor attitude and scale corrections yielded 3-5 cm improvements in the relative accuracy. Once system misalignments were corrected, vertical GPS drift was then resolved and removed per flight line, yielding a slight improvement (<1 cm) in relative accuracy.

The TerraScan software suite is designed specifically for classifying near-ground points (Soininen, 2004). The processing sequence began by 'removing' all points that were not 'near' the earth based on geometric constraints used to evaluate multi-return points. The

resulting bare earth (ground) model was visually inspected and additional ground point modeling was performed in site-specific areas to improve ground detail. This manual editing of ground often occurs in areas with known ground modeling deficiencies, such as: bedrock outcrops, cliffs, deeply incised stream banks, and dense vegetation. In some cases, automated ground point classification erroneously included known vegetation (i.e., understory, low/dense shrubs, etc.). These points were manually reclassified as non-grounds. Ground surface rasters were developed from triangulated irregular networks (TINs) of ground points.

4. LiDAR Accuracy Assessment

Our LiDAR quality assurance process uses the data from the real-time kinematic (RTK) ground survey conducted in the survey area. For both the UTM 10 and UTM 11 areas a cumulative total of **40,266** RTK GPS measurements were collected on hard surfaces distributed among multiple flight swaths. To assess absolute accuracy, we compared the location coordinates of these known RTK ground survey points to those calculated for the closest laser points.

4.1 Laser Noise and Relative Accuracy

Laser point absolute accuracy is largely a function of laser noise and relative accuracy. To minimize these contributions to absolute error, we first performed a number of noise filtering and calibration procedures prior to evaluating absolute accuracy.

Laser Noise

For any given target, laser noise is the breadth of the data cloud per laser return (i.e., last, first, etc.). Lower intensity surfaces (roads, rooftops, still/calm water) experience higher laser noise. The laser noise range for this survey was approximately 0.02 meters.

Relative Accuracy

Relative accuracy refers to the internal consistency of the data set - the ability to place a laser point in the same location over multiple flight lines, GPS conditions, and aircraft attitudes. Affected by system attitude offsets, scale, and GPS/IMU drift, internal consistency is measured as the divergence between points from different flight lines within an overlapping area. Divergence is most apparent when flight lines are opposing. When the LiDAR system is well calibrated, the line-to-line divergence is low (<10 cm). See Appendix A for further information on sources of error and operational measures that can be taken to improve relative accuracy.

Relative Accuracy Calibration Methodology

1. **Manual System Calibration:** Calibration procedures for each mission require solving geometric relationships that relate measured swath-to-swath deviations to misalignments of system attitude parameters. Corrected scale, pitch, roll and heading offsets were calculated and applied to resolve misalignments. The raw divergence between lines was computed after the manual calibration was completed and reported for each survey area.
2. **Automated Attitude Calibration:** All data were tested and calibrated using TerraMatch automated sampling routines. Ground points were classified for each individual flight line and used for line-to-line testing. System misalignment offsets (pitch, roll and heading) and scale were solved for each individual mission and applied to respective

mission datasets. The data from each mission were then blended when imported together to form the entire area of interest.

3. Automated Z Calibration: Ground points per line were used to calculate the vertical divergence between lines caused by vertical GPS drift. Automated Z calibration was the final step employed for relative accuracy calibration.

4.2 Absolute Accuracy

The vertical accuracy of the LiDAR data is described as the mean and standard deviation ($\sigma \sim \sigma$) of divergence of LiDAR point coordinates from RTK ground survey point coordinates. To provide a sense of the model predictive power of the dataset, the root mean square error (RMSE) for vertical accuracy is also provided. These statistics assume the error distributions for x, y, and z are normally distributed, thus we also consider the skew and kurtosis of distributions when evaluating error statistics.

Statements of statistical accuracy apply to fixed terrestrial surfaces only and may not be applied to areas of dense vegetation or steep terrain (See Appendix A). To calibrate laser accuracy for the Delivery 12 LiDAR dataset 509 RTK points were collected in UTM 11 on fixed, hard-packed road surfaces within the survey area.

5. Study Area Results

Summary statistics for point resolution and accuracy (relative and absolute) of the LiDAR data collected in the Columbia River survey areas are presented below in terms of central tendency, variation around the mean, and the spatial distribution of the data (for point resolution by quadrangle).

5.1 Data Summary

Table 3. Resolution and Accuracy - Specifications and Achieved Values reported by UTM zone

	Targeted	Achieved	Achieved (without water)
Resolution:			
UTM10	≥ 8 points/m ²	7.23 points/m ²	8.94 points/m ²
UTM 11	≥ 8 points/m ²	6.08 points/m ²	8.63 point/m ²
*Vertical Accuracy (1 σ):			
UTM10	<13 cm	4.4 cm	
UTM 11	<13 cm	4.7 cm	

* Based on 11,440 hard-surface control points collected within UTM 10 and 28,826 hard-surface control points collected within UTM 11.

Table 4. Resolution and Accuracy - Specifications and achieved values for the total project area

	Targeted	Achieved
Resolution:	≥ 8 points/m ²	8.76 points/m ²
*Vertical Accuracy (1 σ):	<13 cm	4.6 cm
Relative Accuracy		0.035 cm

5.2 Data Density/Resolution

With areas of water removed from calculations, the average first-return density of the UTM 10 and UTM 11 delivered datasets are 8.94 and 8.63 points per square meter respectively (**Table 3**) with a total project average of 8.76 points per square meter. The initial dataset, acquired to be 8 points per square meter, was filtered as described previously to remove spurious or inaccurate points. Additionally, some types of surfaces (i.e., dense vegetation, breaks in terrain, water, steep slopes) may return fewer pulses (delivered density) than the laser originally emitted (native density). Water area was calculated from breakline shapes created by DSA. Final native density numbers were calculated with water area subtracted from total project area and first return points within the water area subtracted from the total point count to provide a more accurate density over land.

Ground classifications were derived from automated ground surface modeling and manual, supervised classifications where it was determined that the automated model had failed. Ground return densities will be lower in areas of dense vegetation, water, or buildings. The maps in **Figures 7 - 34** identify the average native and ground point densities for each USGS 0.75 minute quad. Tiles with greater than 20 million points were divided in half to keep LAS file sizes manageable.

Cumulative LiDAR data resolution for UTM 10 of the Columbia River survey without water adjustment:

- Average Point (First Return) Density = 7.23 points/m²
- Average Ground Point Density = 1.10 points/m²

Figure 3. Density distribution for first return laser points in UTM 10.

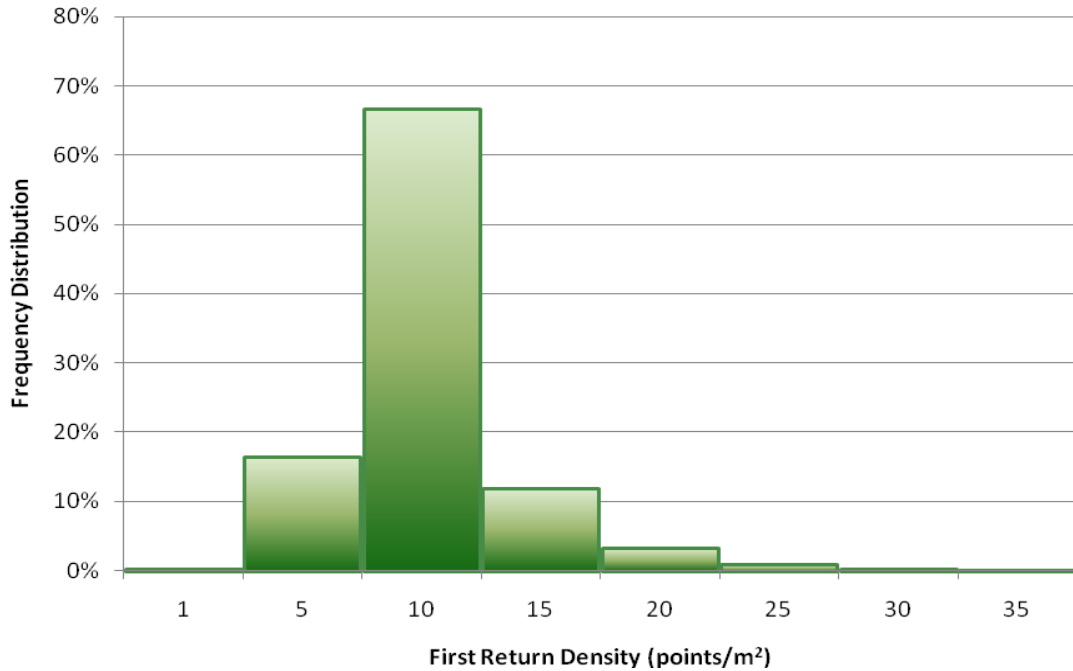
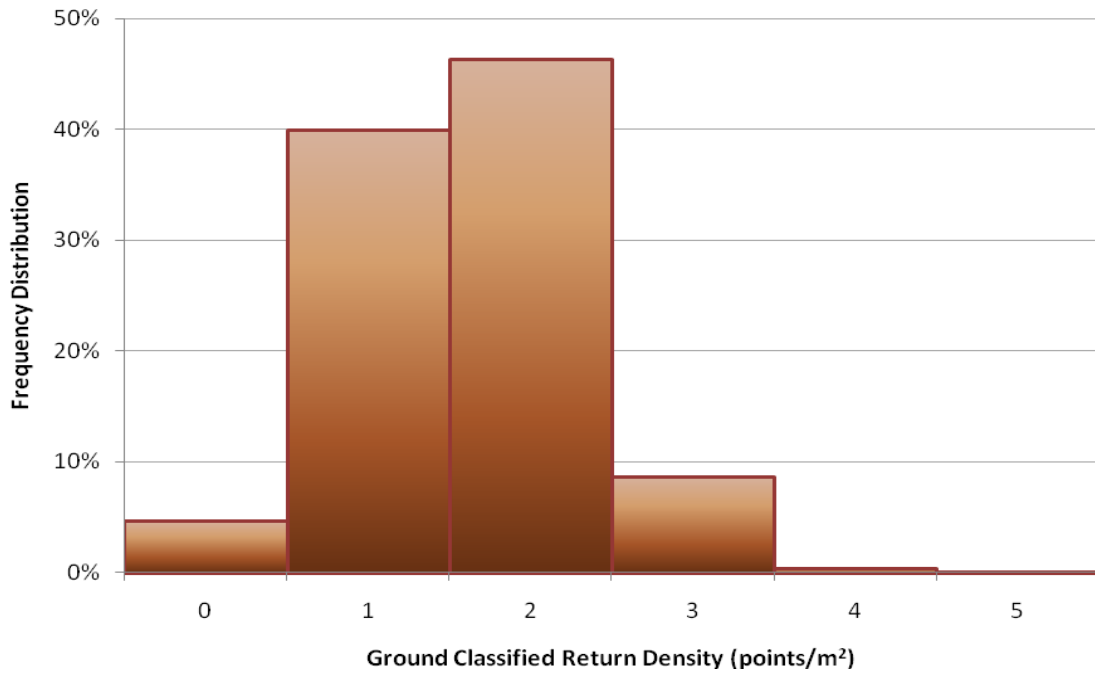


Figure 4. Density distribution for ground classified laser points in, UTM 10.



Cumulative LiDAR data resolution for UTM 11 of the Columbia River survey without water adjustment:

- Average Point (First Return) Density = 6.08 points/m²
- Average Ground Point Density = 1.56 points/m²

Figure 5. Density distribution for first return laser points in UTM 11.

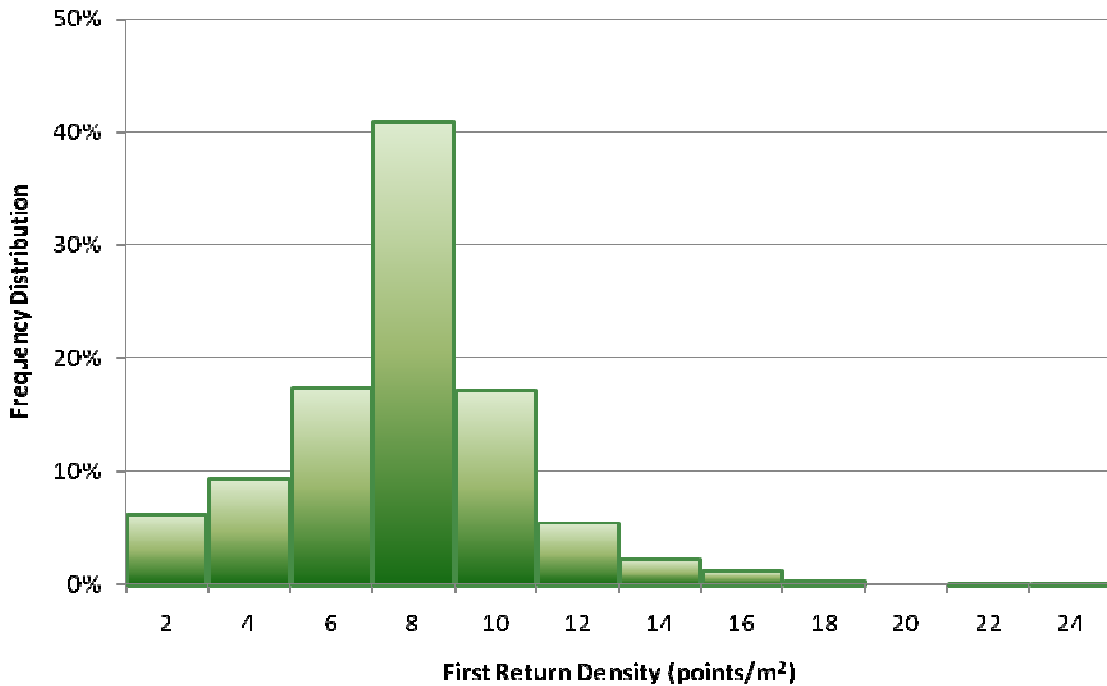


Figure 6. Density distribution for ground classified laser points in, UTM 11.

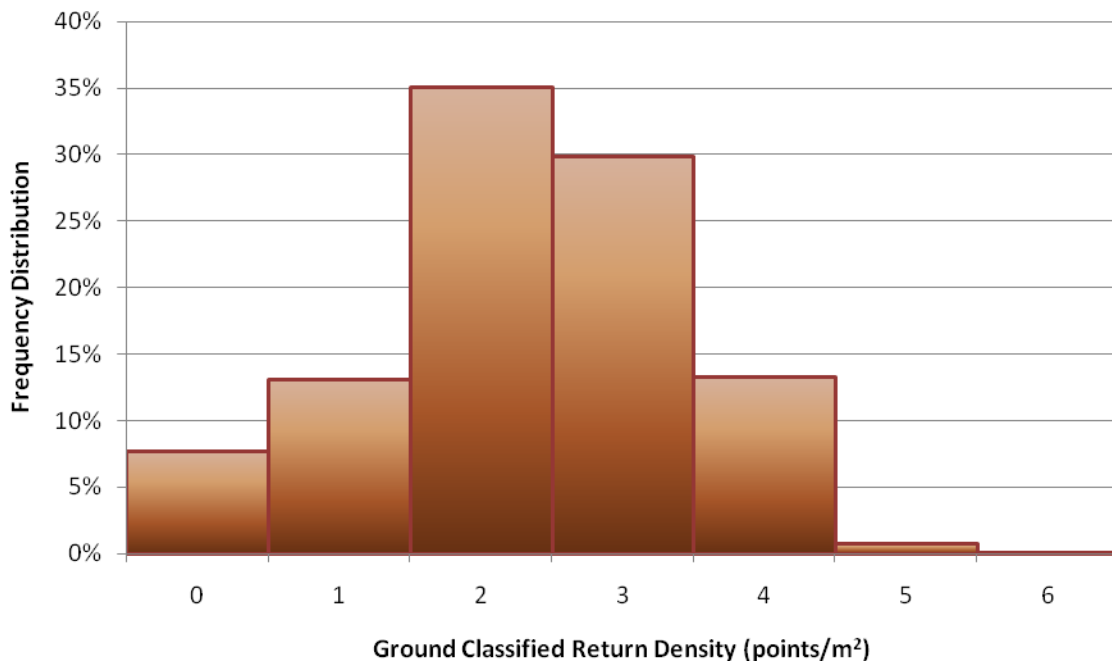


Figure 7. Delivery 1, UTM 10 density distribution map for first return points by USGS 0.75 minute quads.

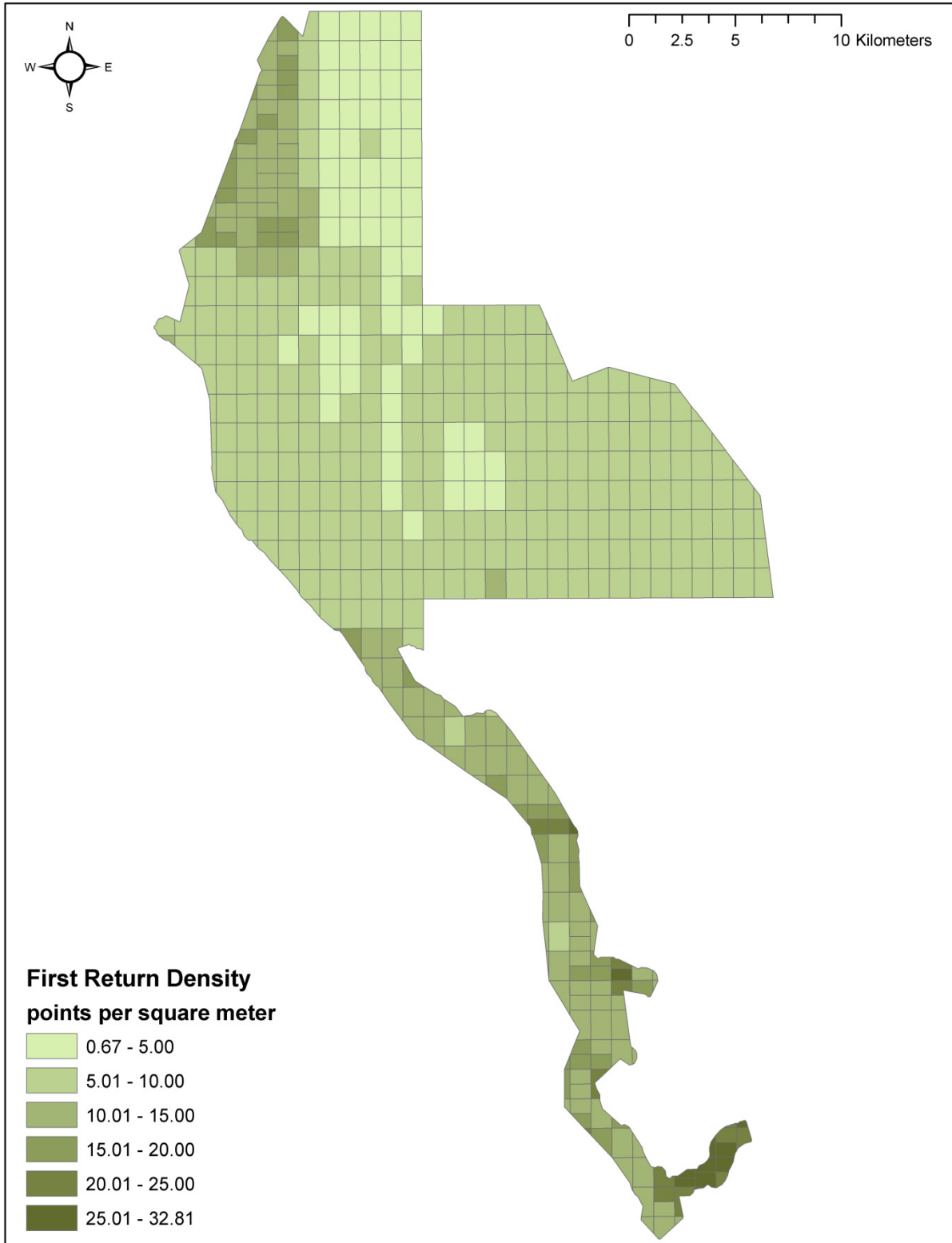


Figure 8. Delivery 1, UTM 10 density distribution map for ground return points by USGS 0.75 minute quads.

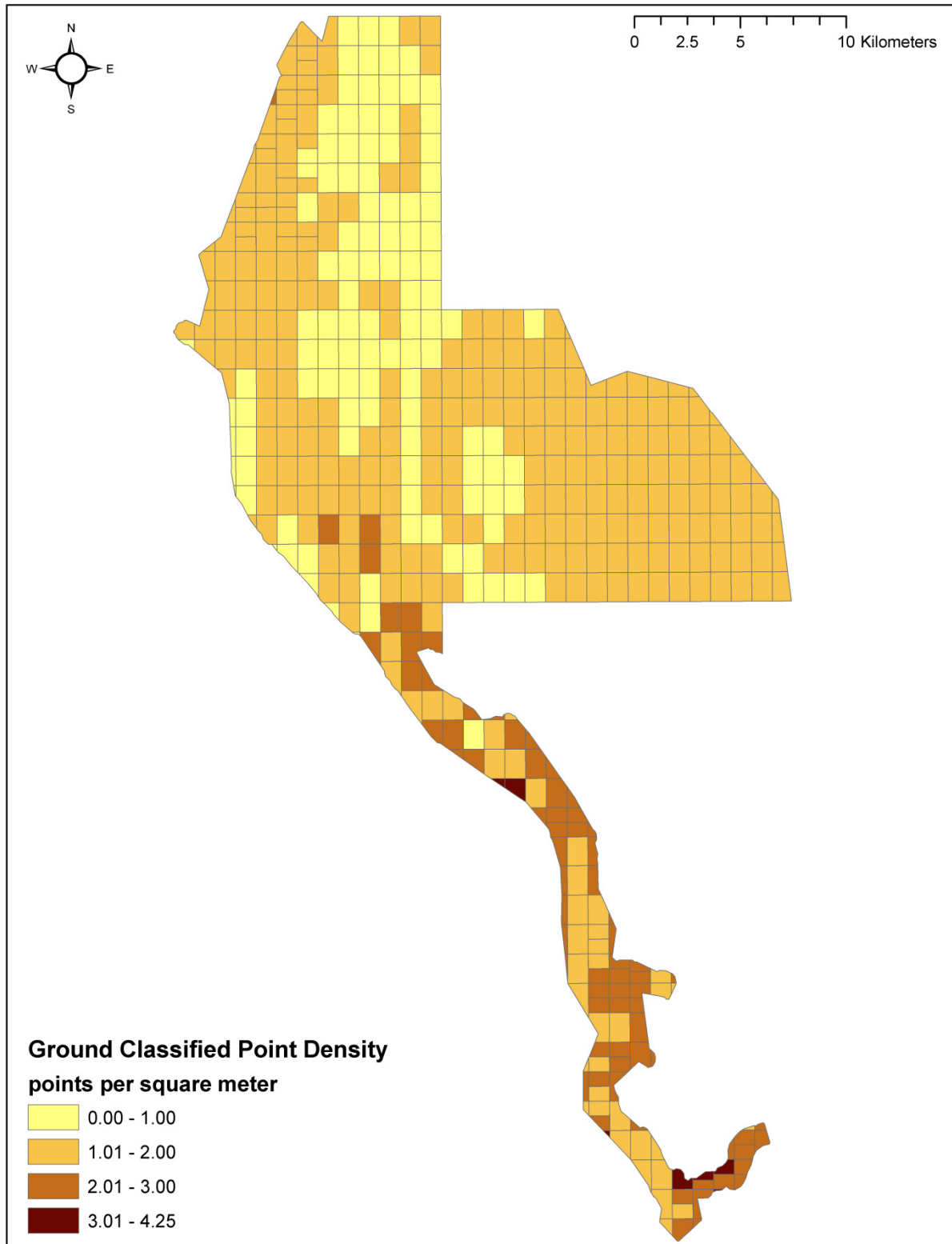


Figure 9. Delivery 1, UTM 11 density distribution map for first return points by USGS 0.75 minute quads.

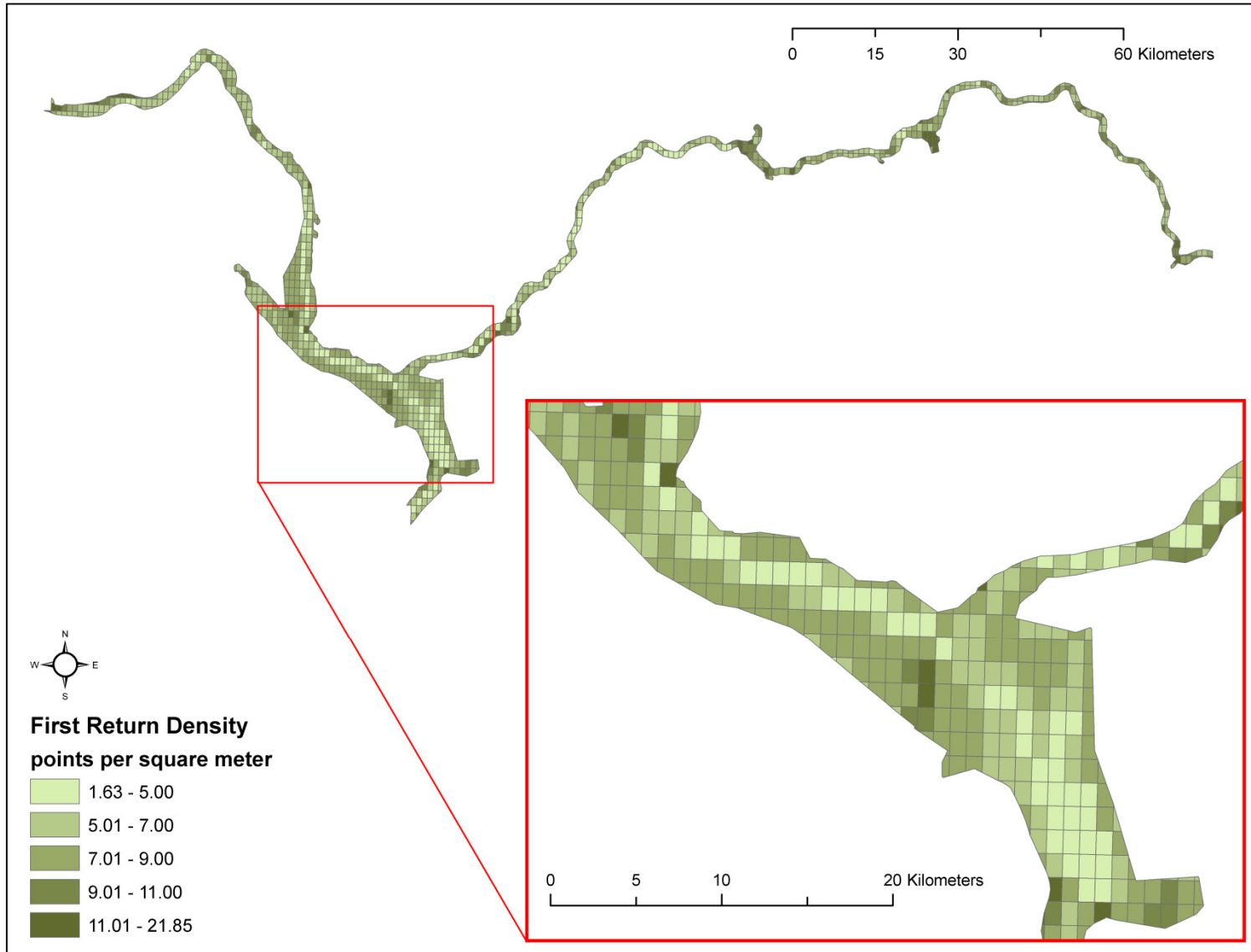


Figure 10. Delivery 1, UTM 11 density distribution map for ground return points by USGS 0.75 minute quads.

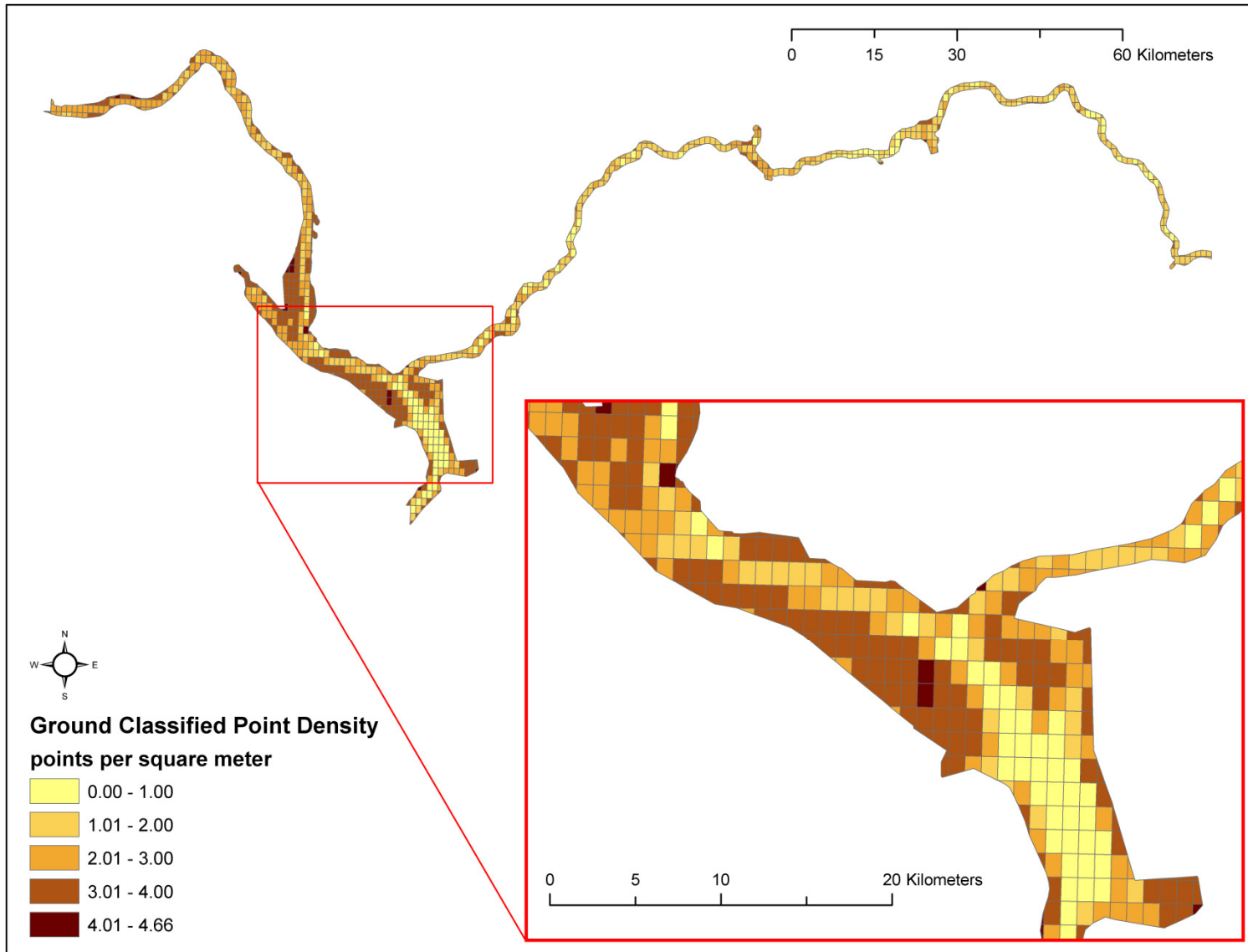


Figure 11. Delivery 2, UTM 10 density distribution map for first return points by USGS 0.75 minute quads.

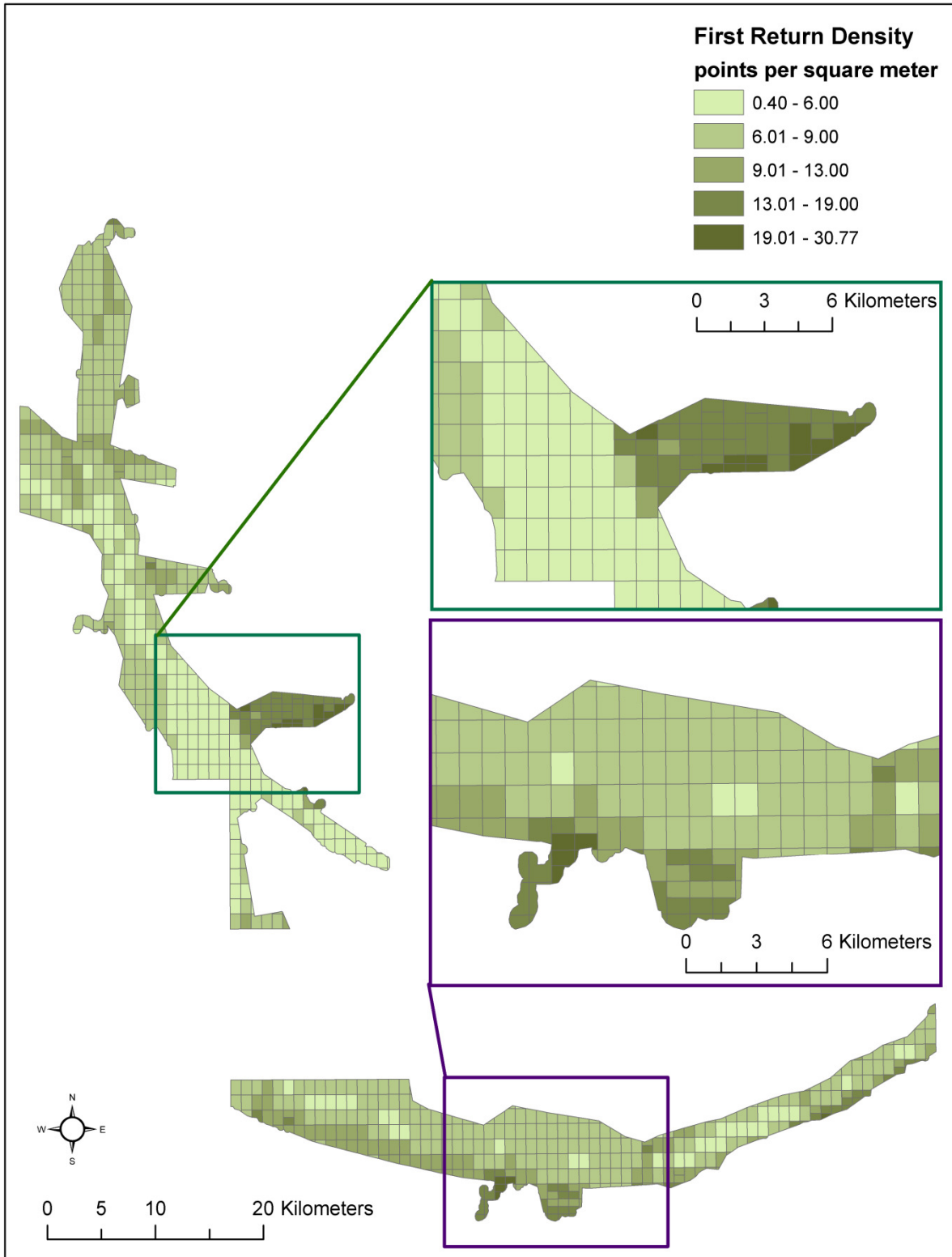


Figure 12. Delivery 2, UTM 10 density distribution map for ground return points by USGS 0.75 minute quads.

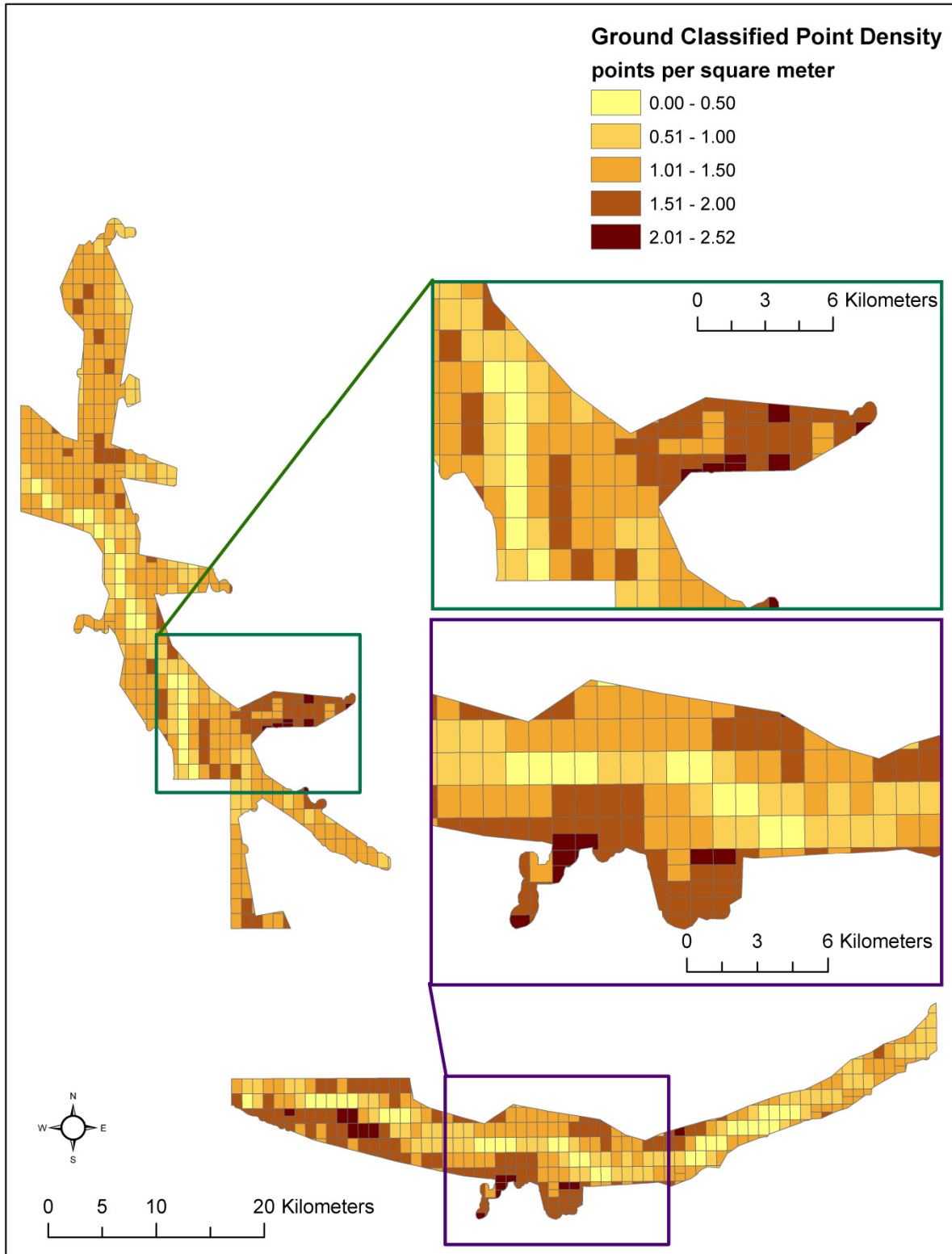


Figure 13. Delivery 3, UTM 11 density distribution map for first return points by USGS 0.75 minute quads

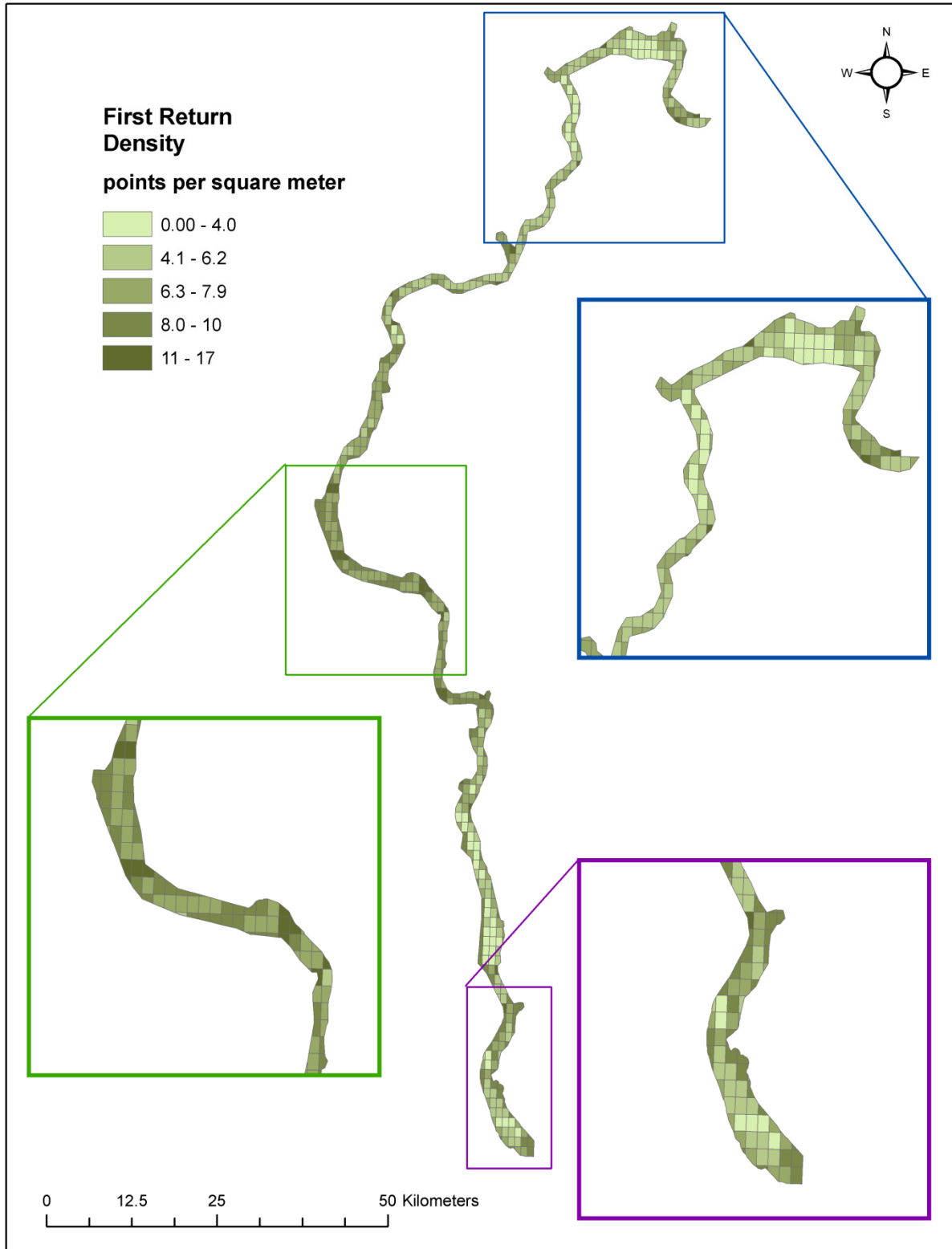


Figure 14. Delivery 3, UTM 11 density distribution map for ground return points by USGS 0.75 minute quads.

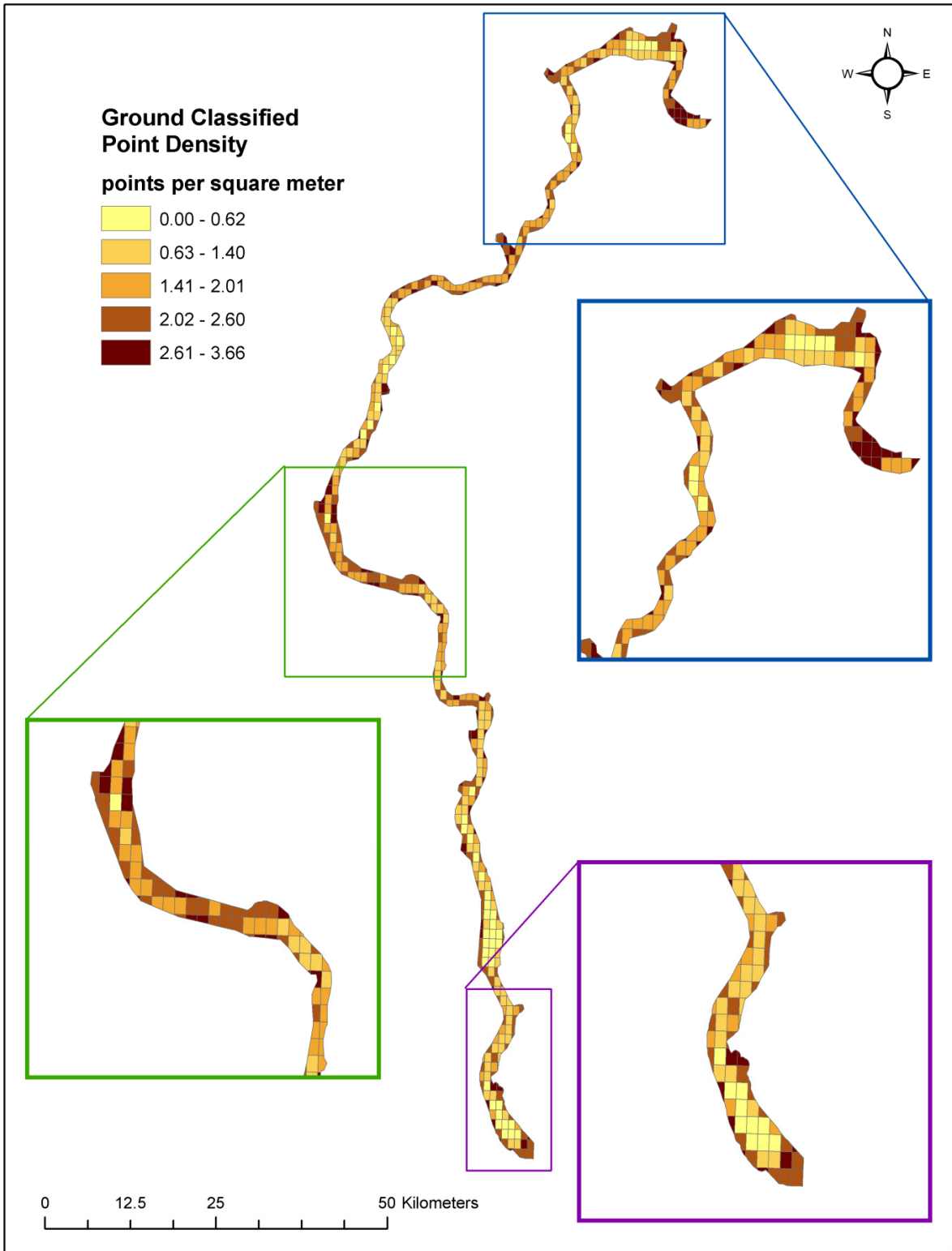


Figure 15. Delivery 4, UTM 10 density distribution map for first return points by USGS 0.75 minute quads.

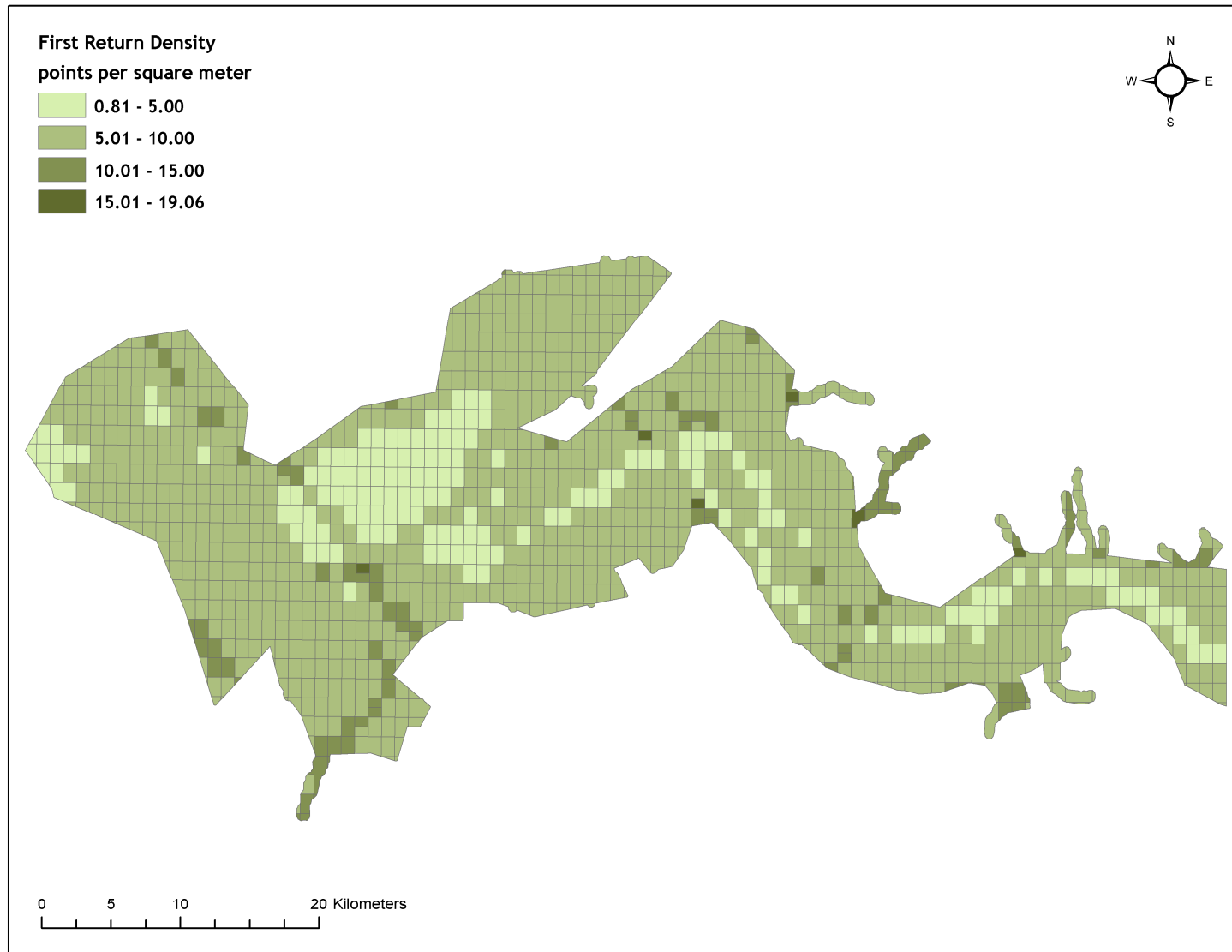


Figure 16. Delivery 4, UTM 10 density distribution map for ground return points by USGS 0.75 minute quads.

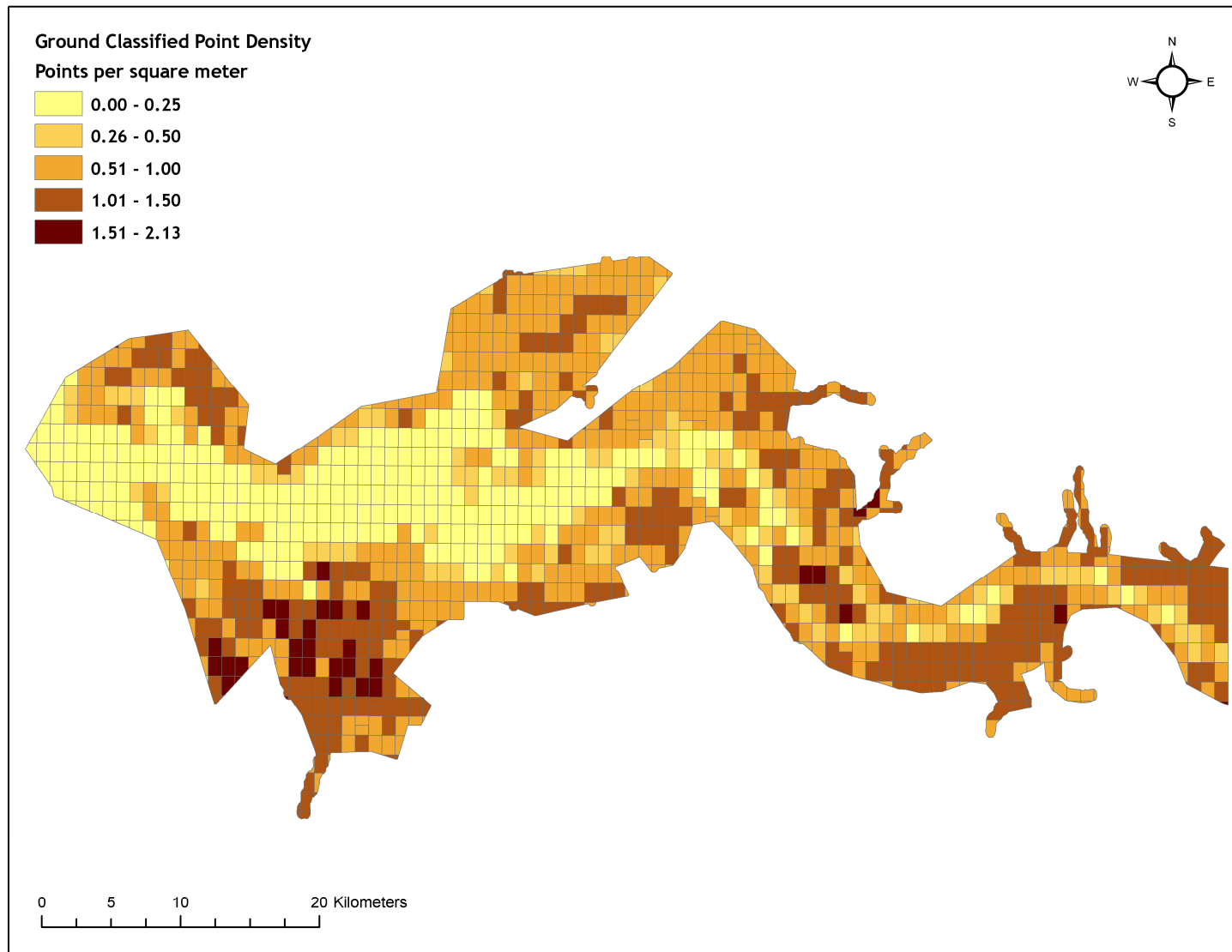


Figure 17. Delivery 5, UTM 11 density distribution map for first return points by USGS 0.75 minute quads.

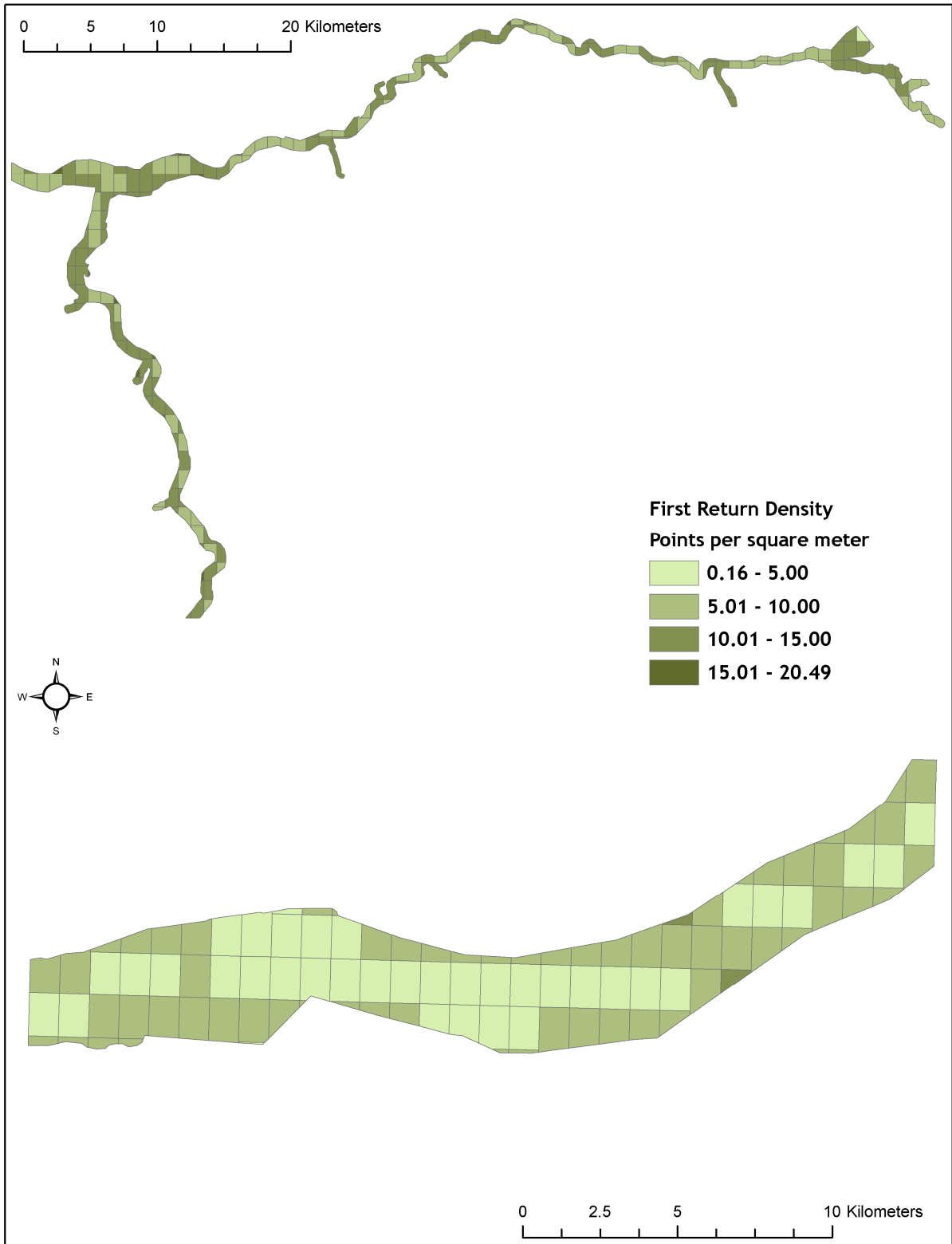


Figure 18. Delivery 5, UTM 11 density distribution map for ground classified points by USGS 0.75 minute quads.

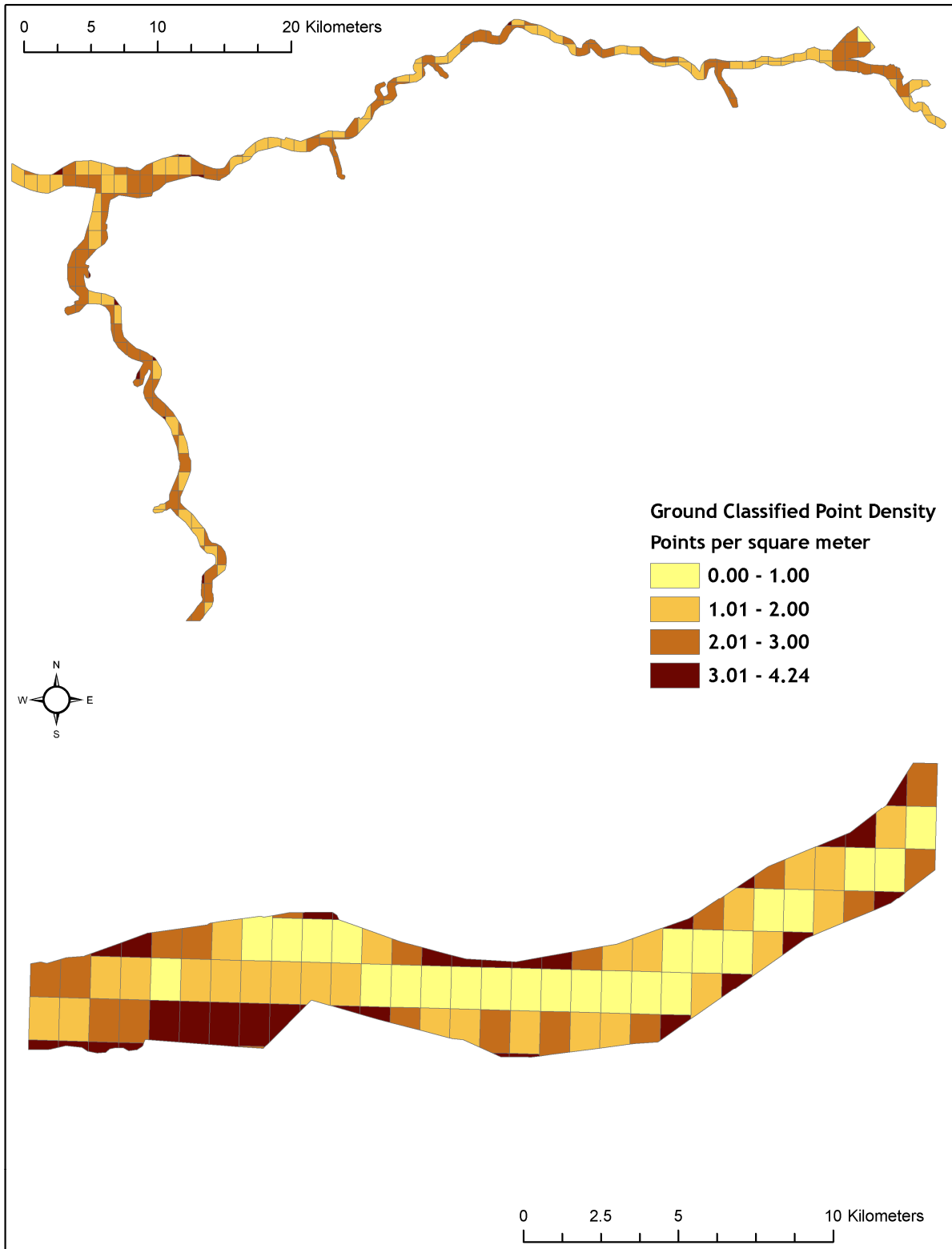


Figure 19. Delivery 6, UTM 11 density distribution map for first return points by USGS 0.75 minute quads.

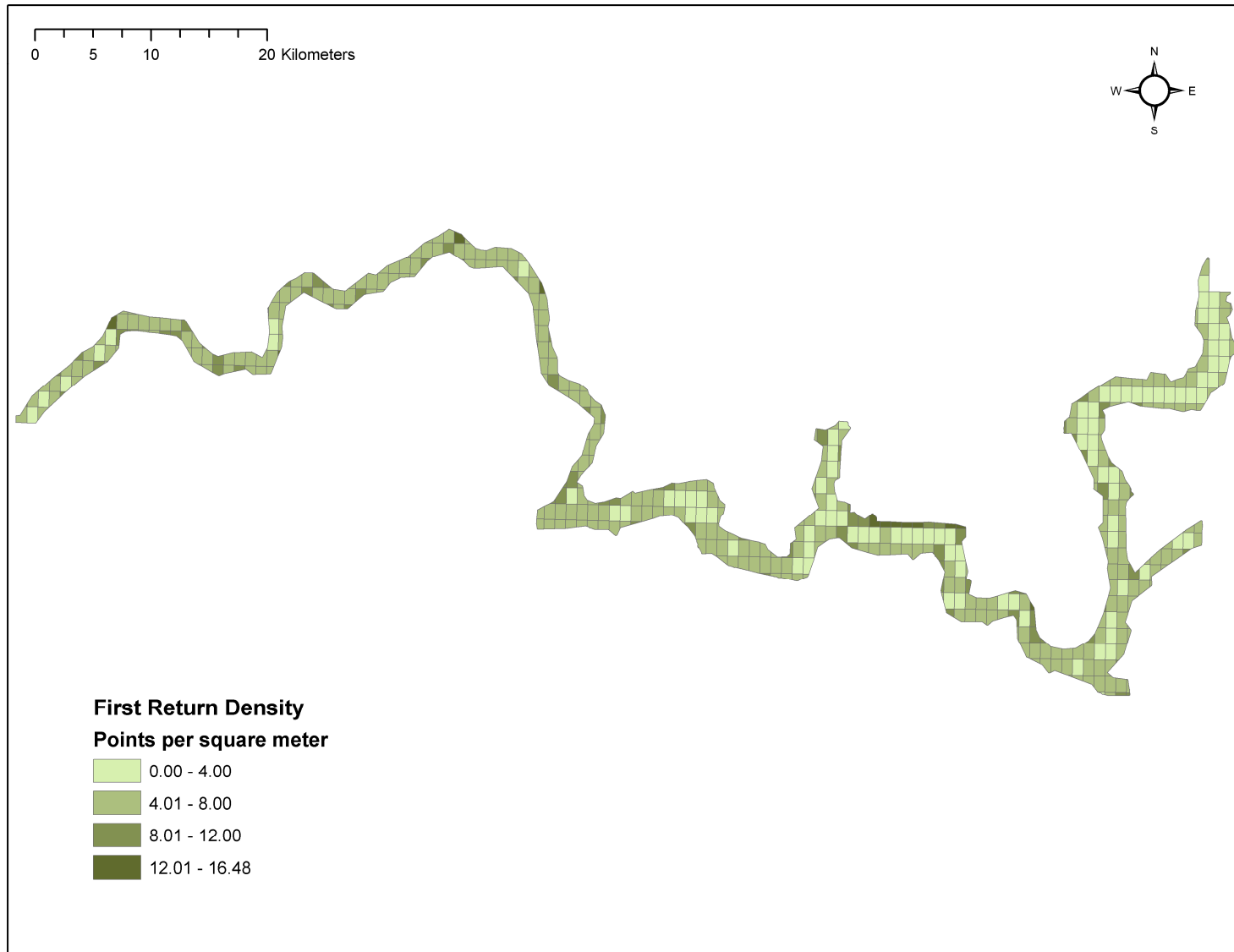


Figure 20. Delivery 6, UTM 11 density distribution map for ground classified points by USGS 0.75 minute quads.

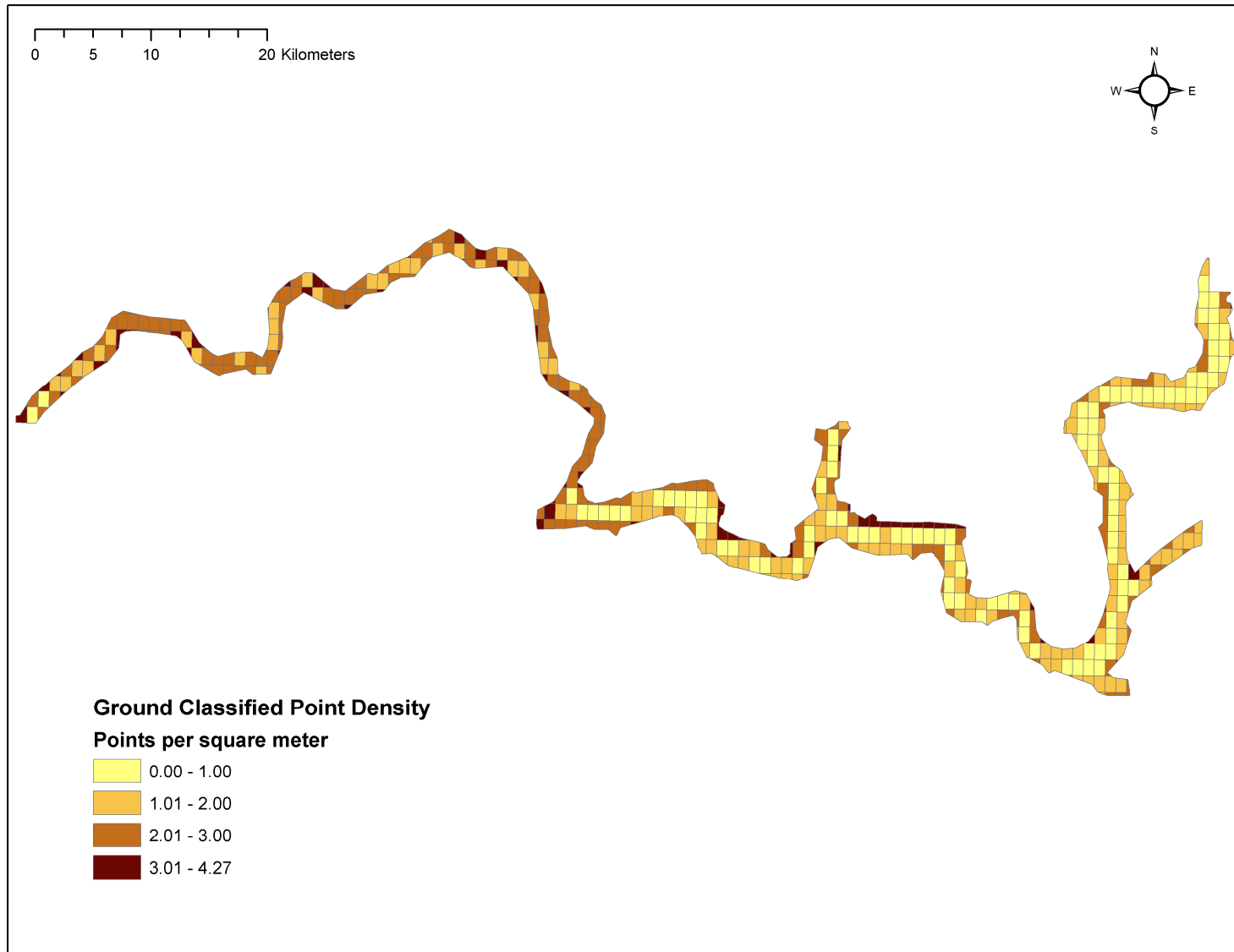


Figure 21. Delivery 6b, UTM 11 density distribution map for first return points by USGS 0.75 minute quads.

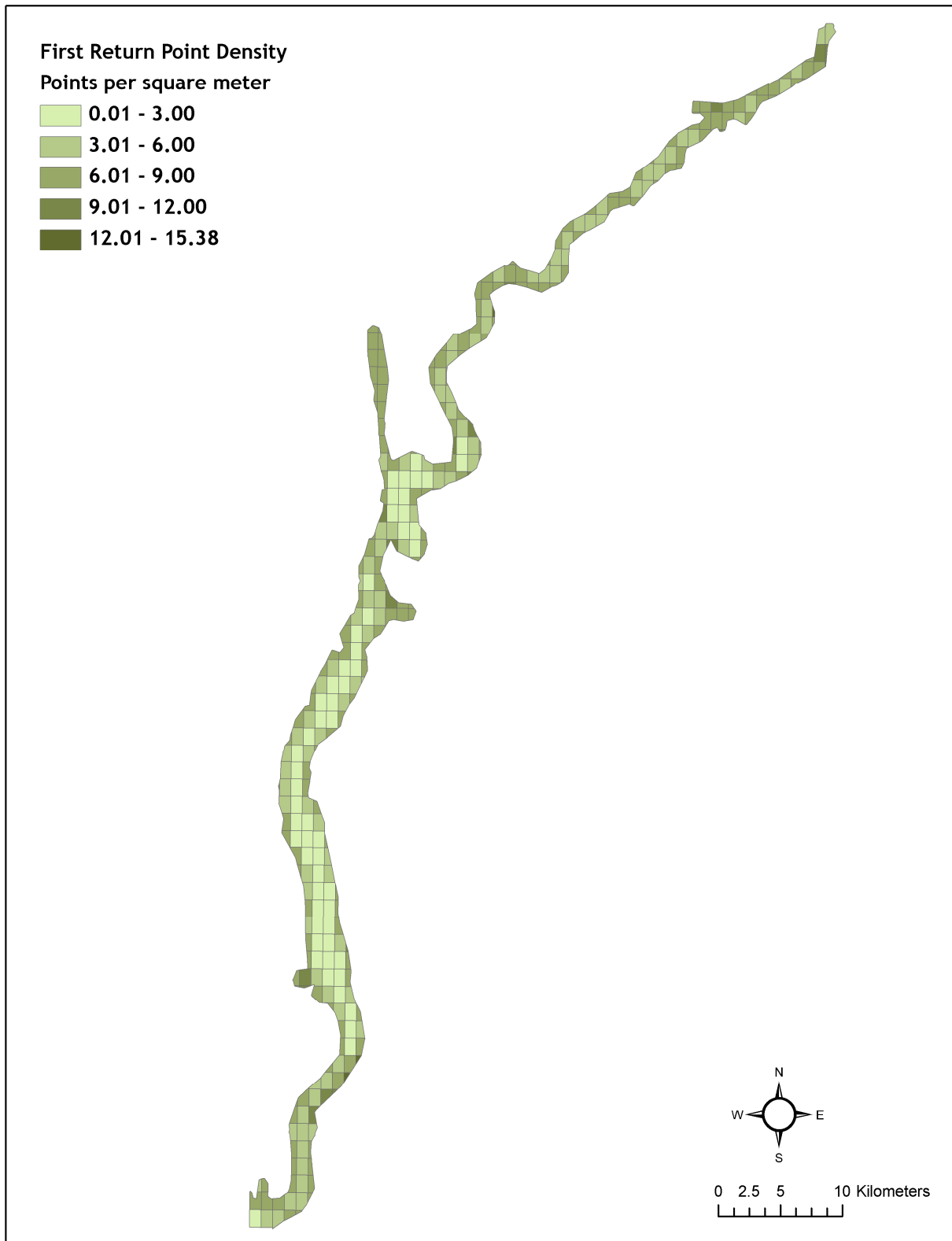


Figure 22. Delivery 6b, UTM 11 density distribution map for ground classified points by USGS 0.75 minute quads.

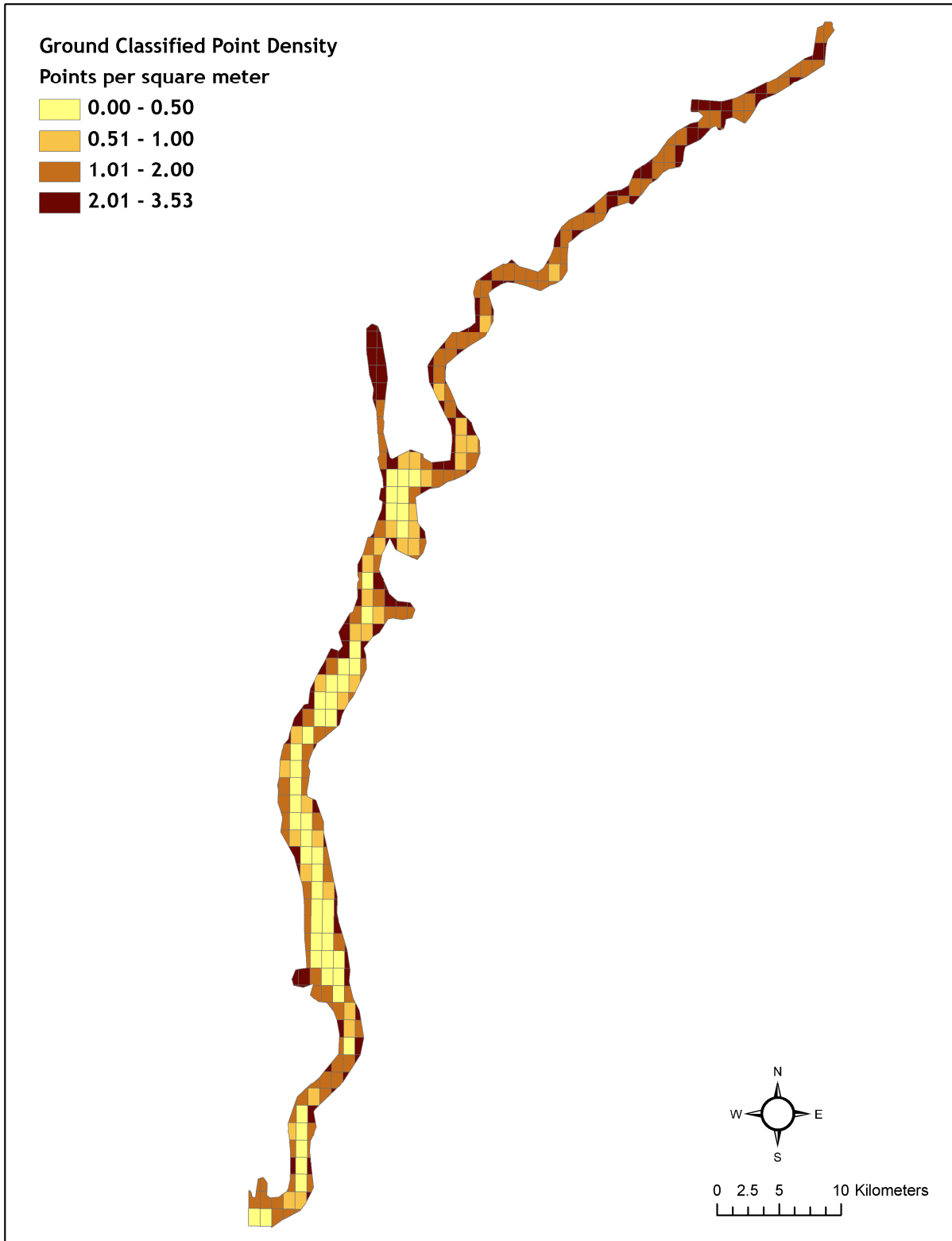


Figure 23. Delivery 7, UTM 11 density distribution map for first return points by USGS 0.75 minute quads.

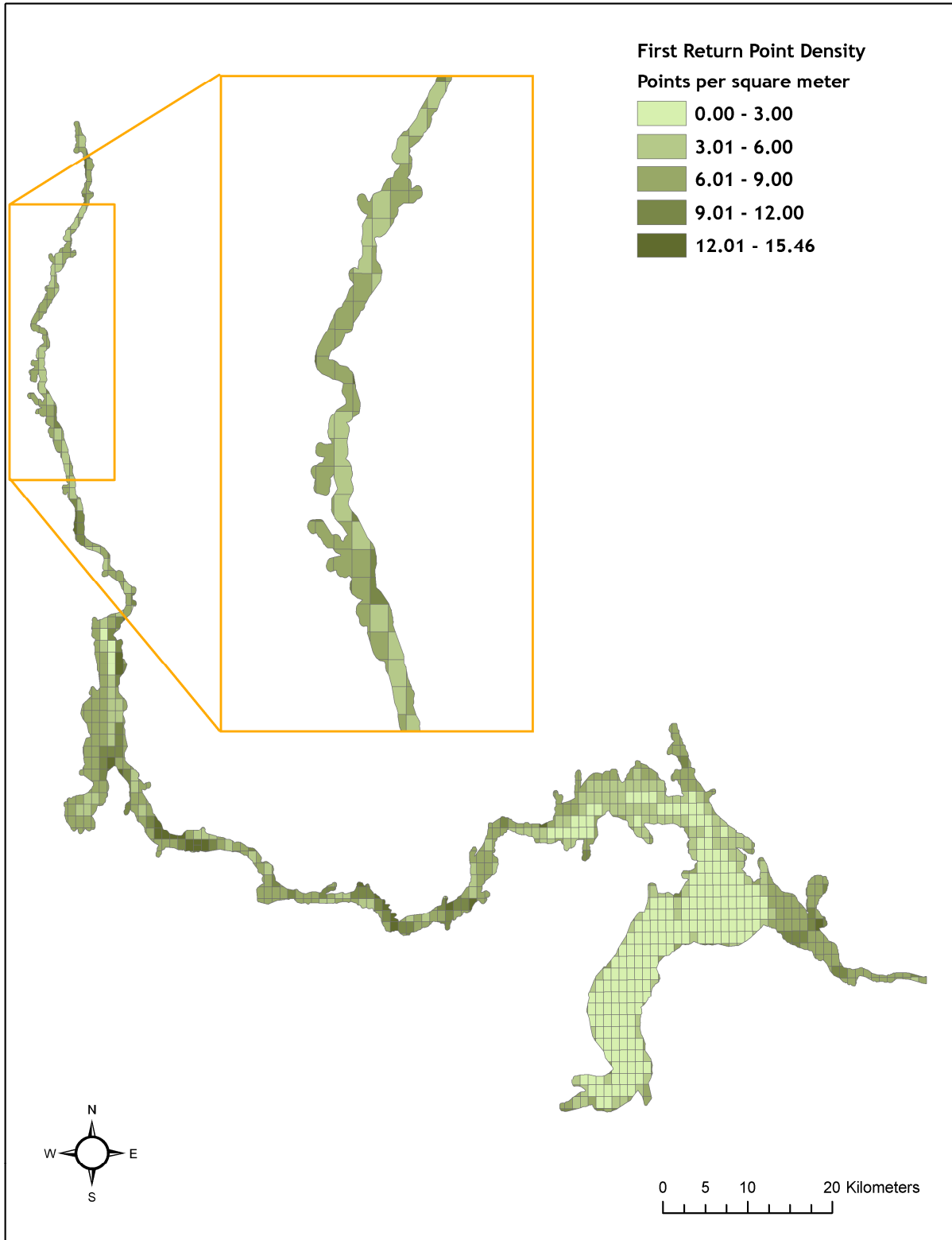


Figure 24. Delivery 7, UTM 11 density distribution map for ground classified points by USGS 0.75 minute quads.

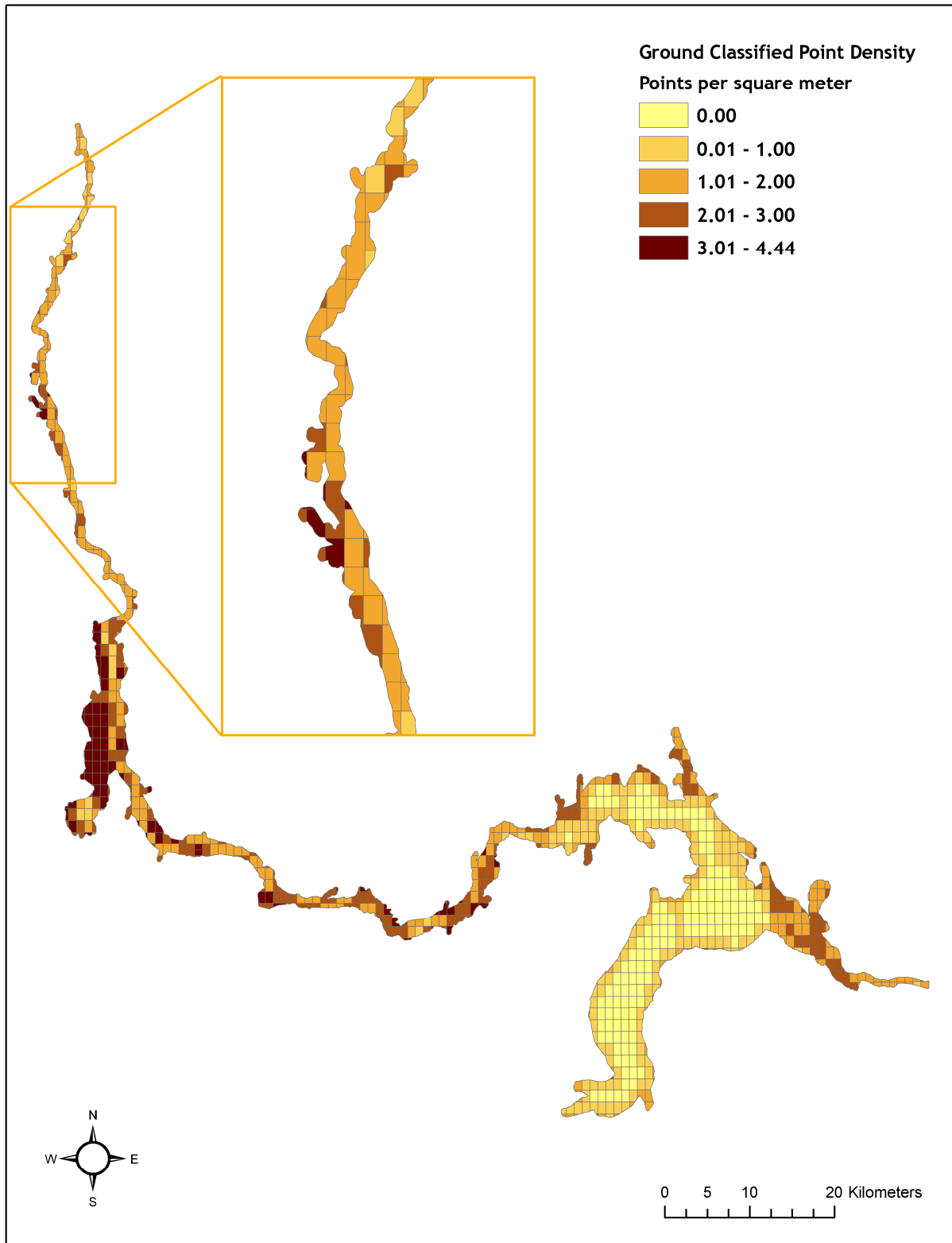


Figure 25. Delivery 8, UTM 10 density distribution map for ground classified and first return points by USGS 0.75 minute quads.

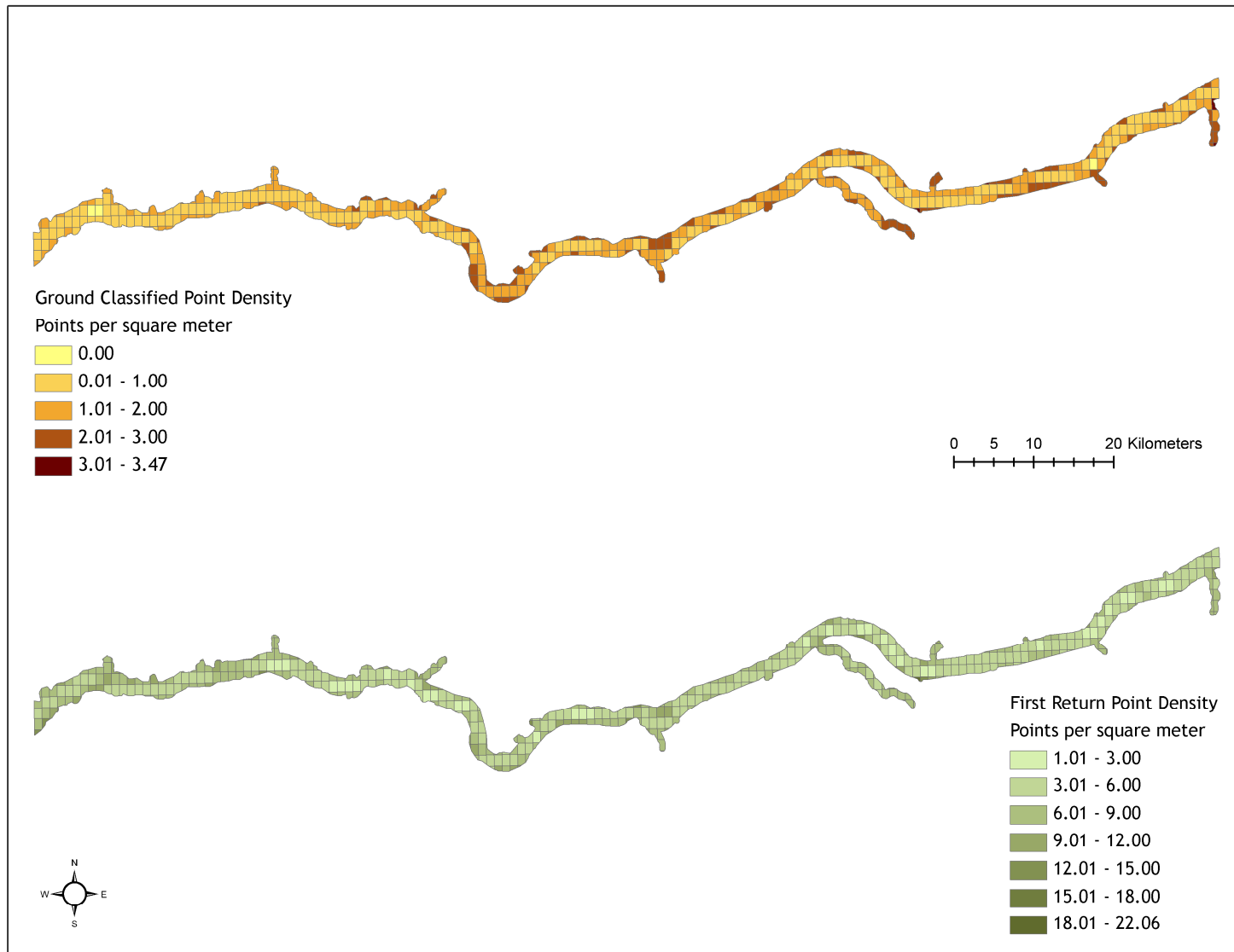


Figure 26. Delivery 8, UTM 11 density distribution map for ground classified and first return points by USGS 0.75 minute quads.

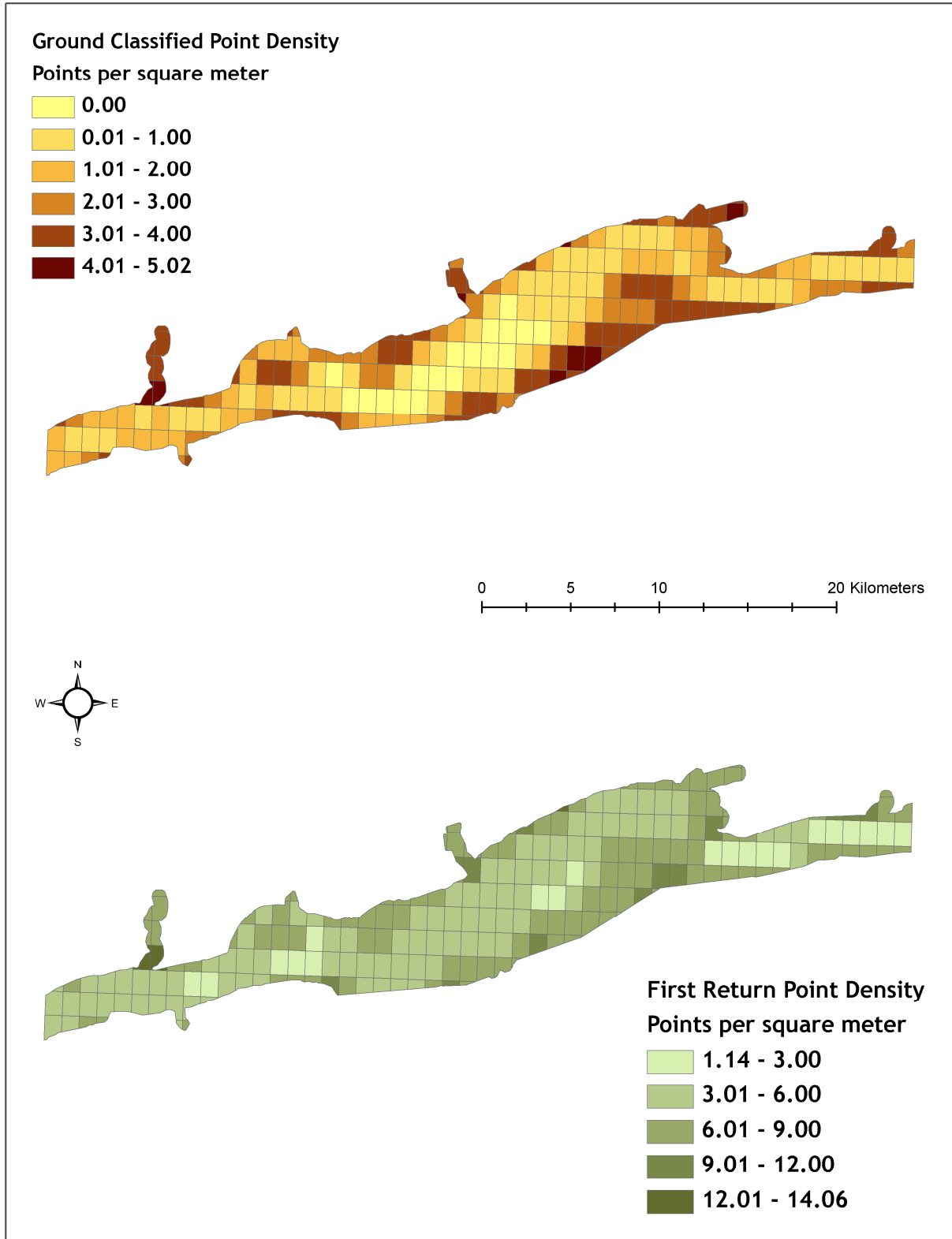


Figure 27. Delivery 9, UTM 11 density distribution map for first return points by USGS 0.75 minute quads.

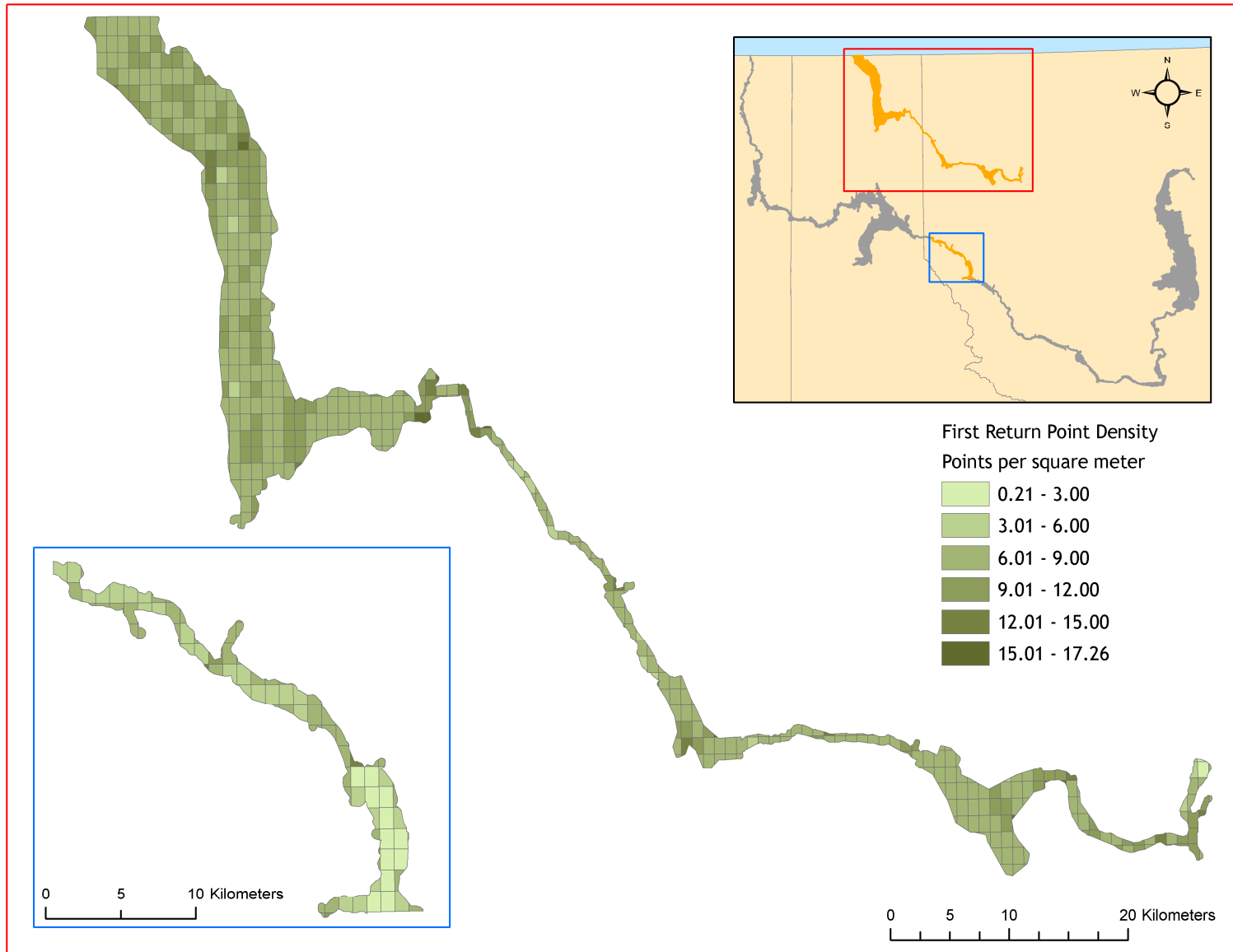


Figure 28. Delivery 9, UTM 11 density distribution map for ground classified points by USGS 0.75 minute quads.

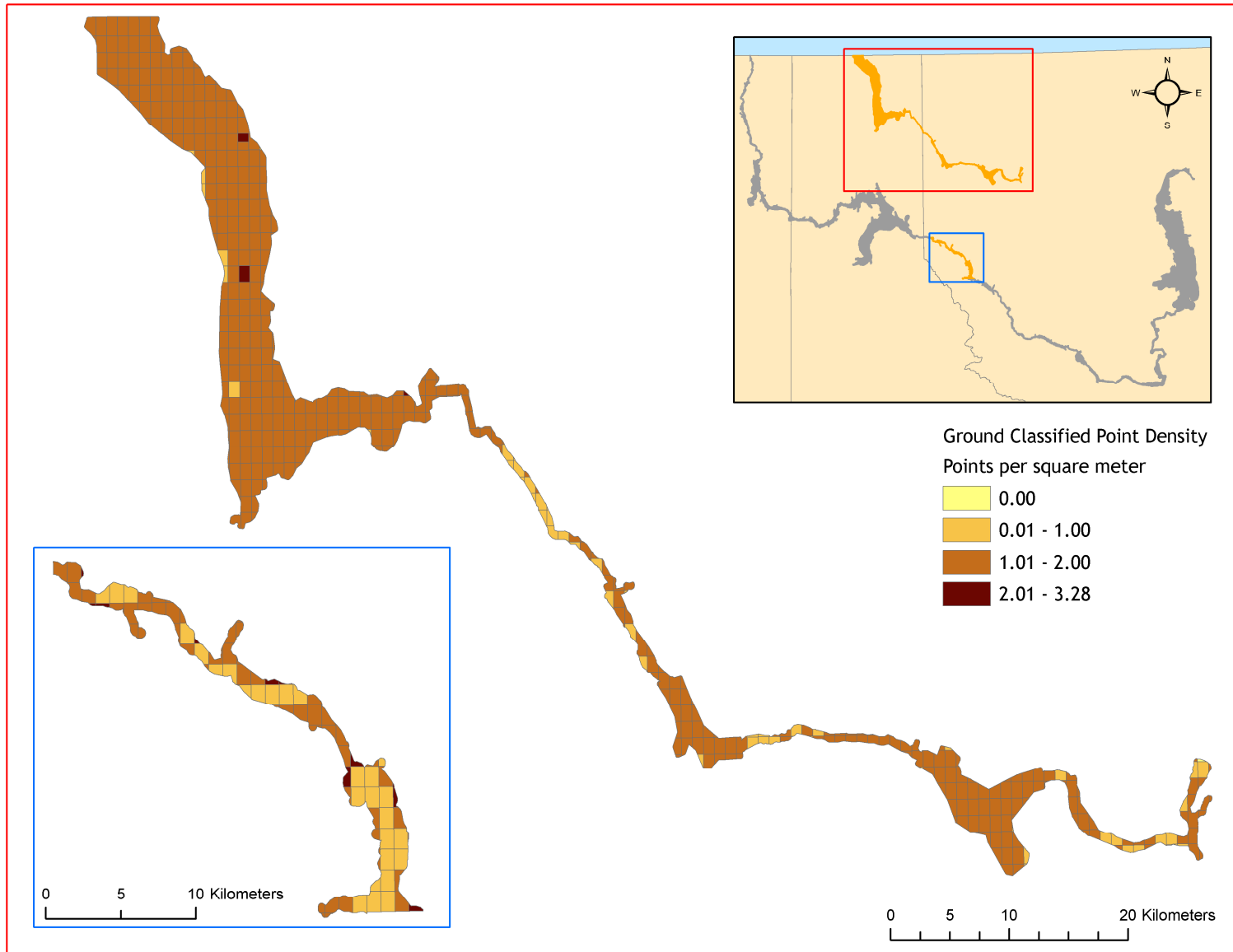


Figure 29. Delivery 10, UTM 11 density distribution map for first return points by USGS 0.75 minute quads.

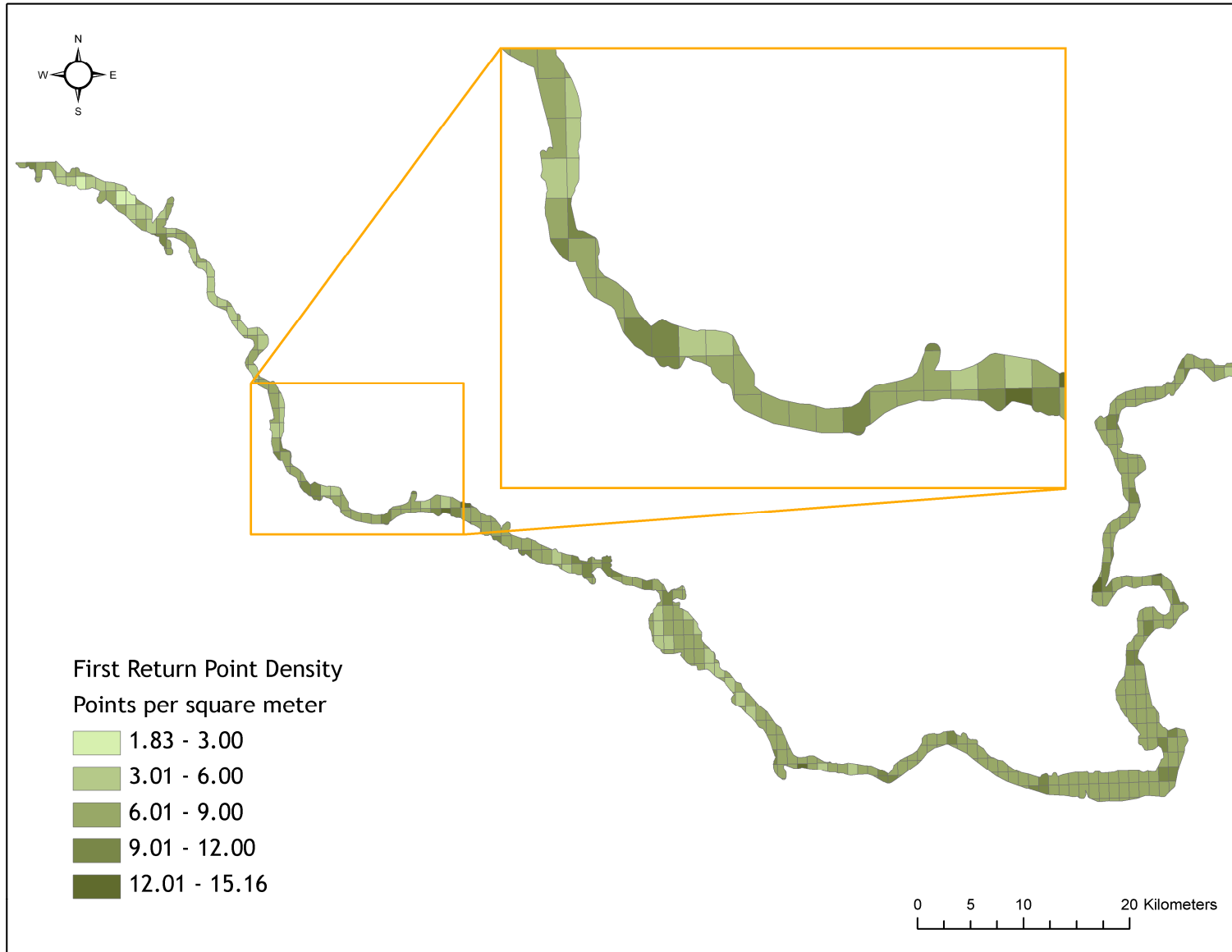


Figure 30. Delivery 10, UTM 11 density distribution map for ground classified points by USGS 0.75 minute quads.

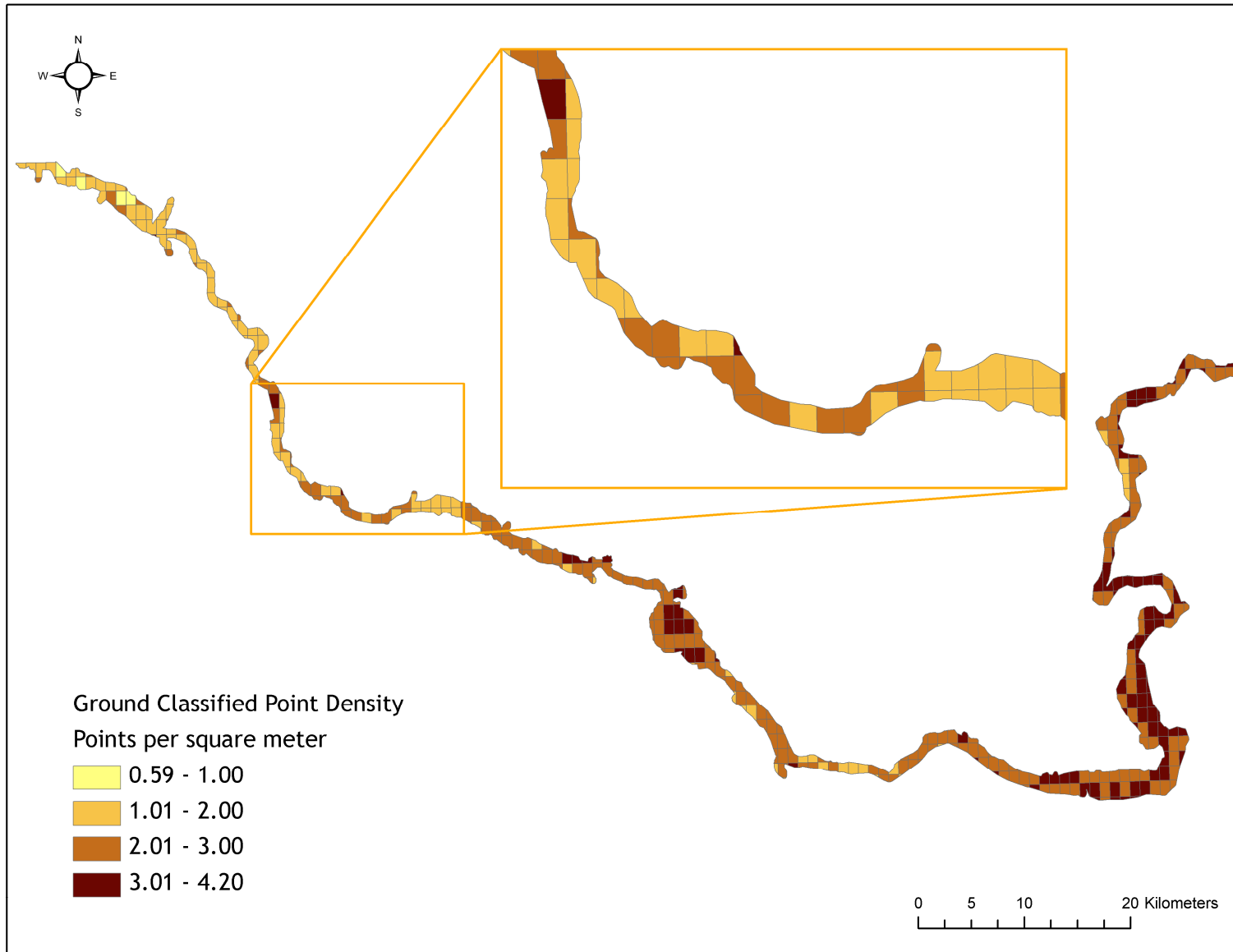


Figure 31. Delivery 11, UTM 11 density distribution map for first return points by USGS 0.75 minute quads.

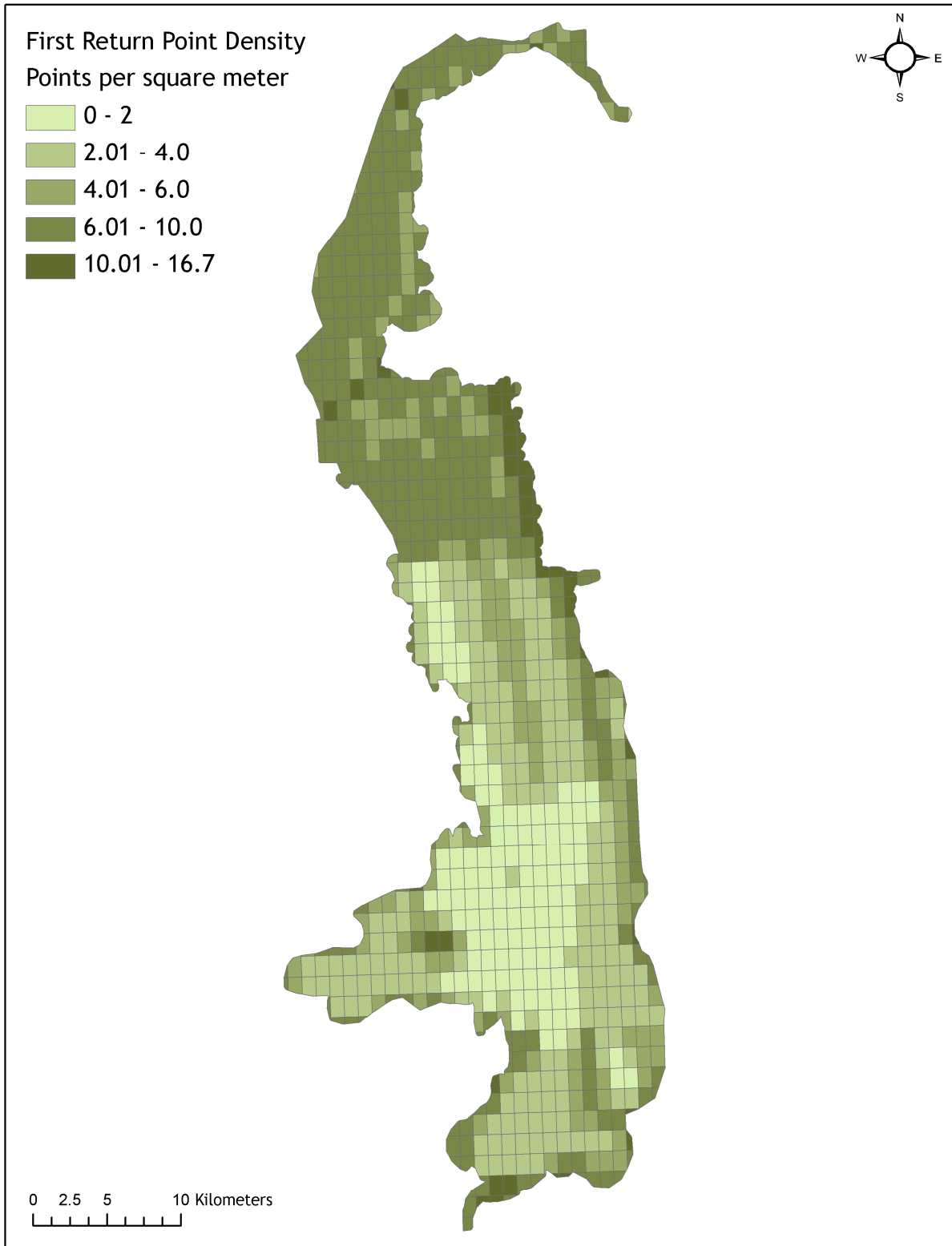


Figure 32. Delivery 11, UTM 11 density distribution map for ground classified points by USGS 0.75 minute quads.

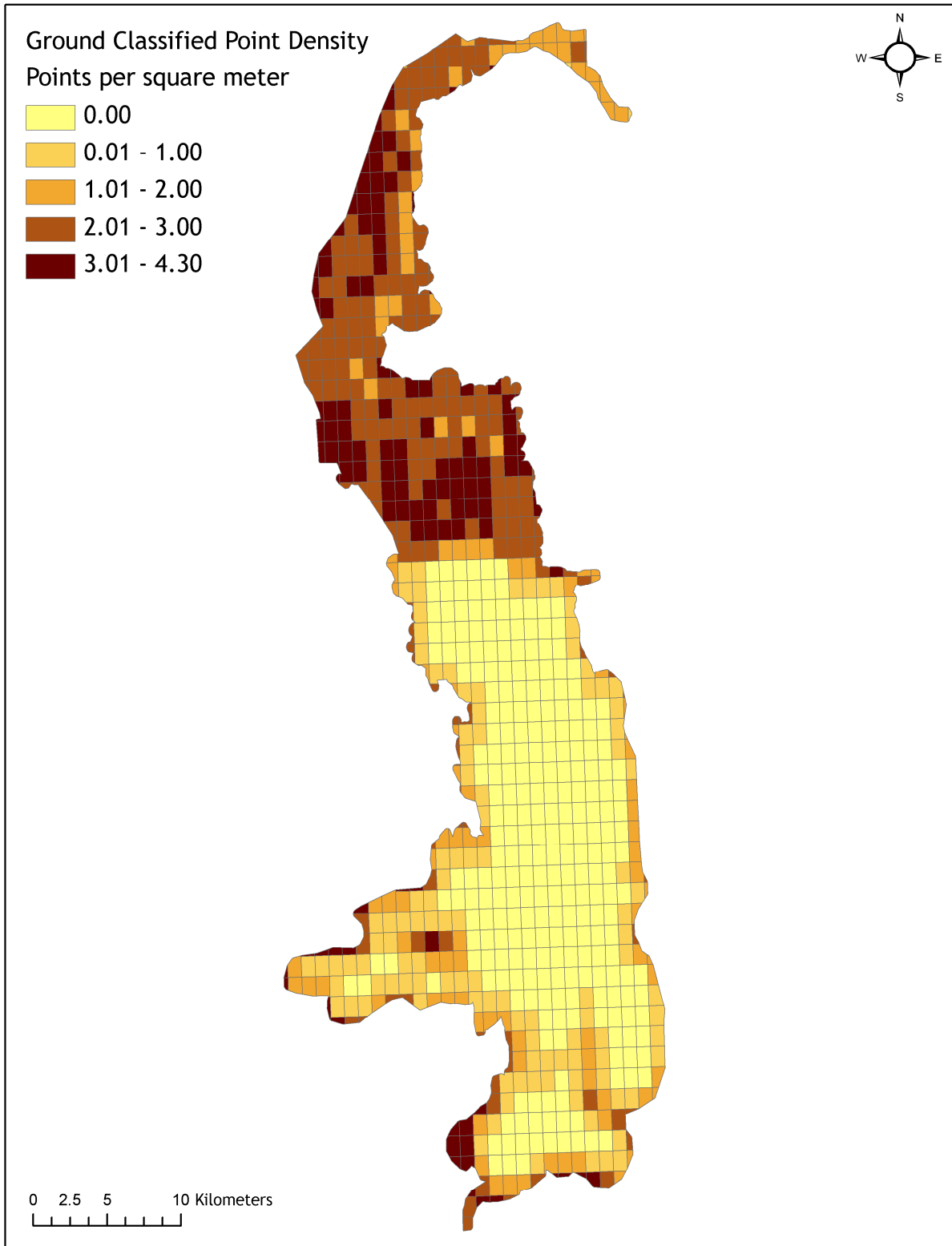


Figure 33. Delivery 12, UTM 11 density distribution map for first return points by USGS 0.75 minute quads.

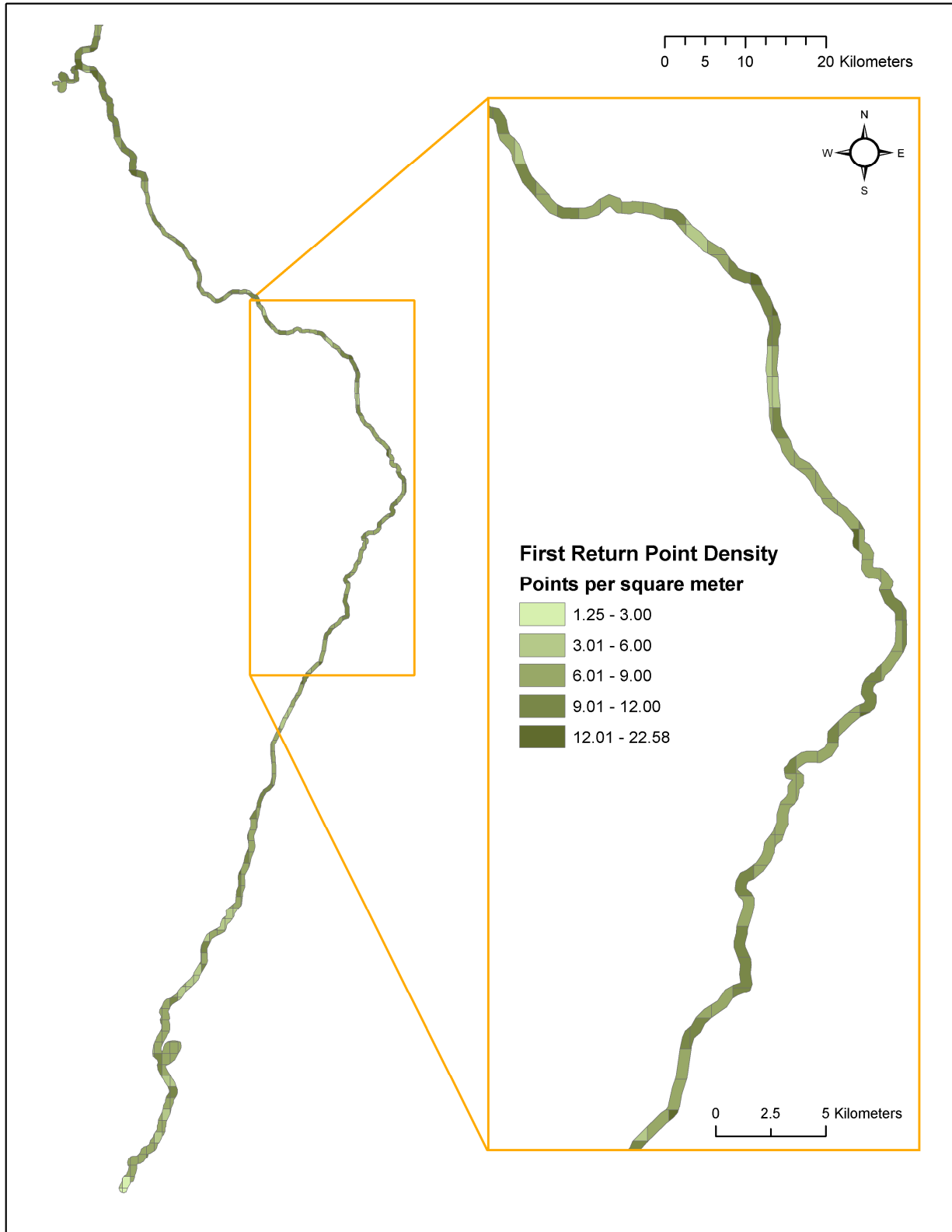
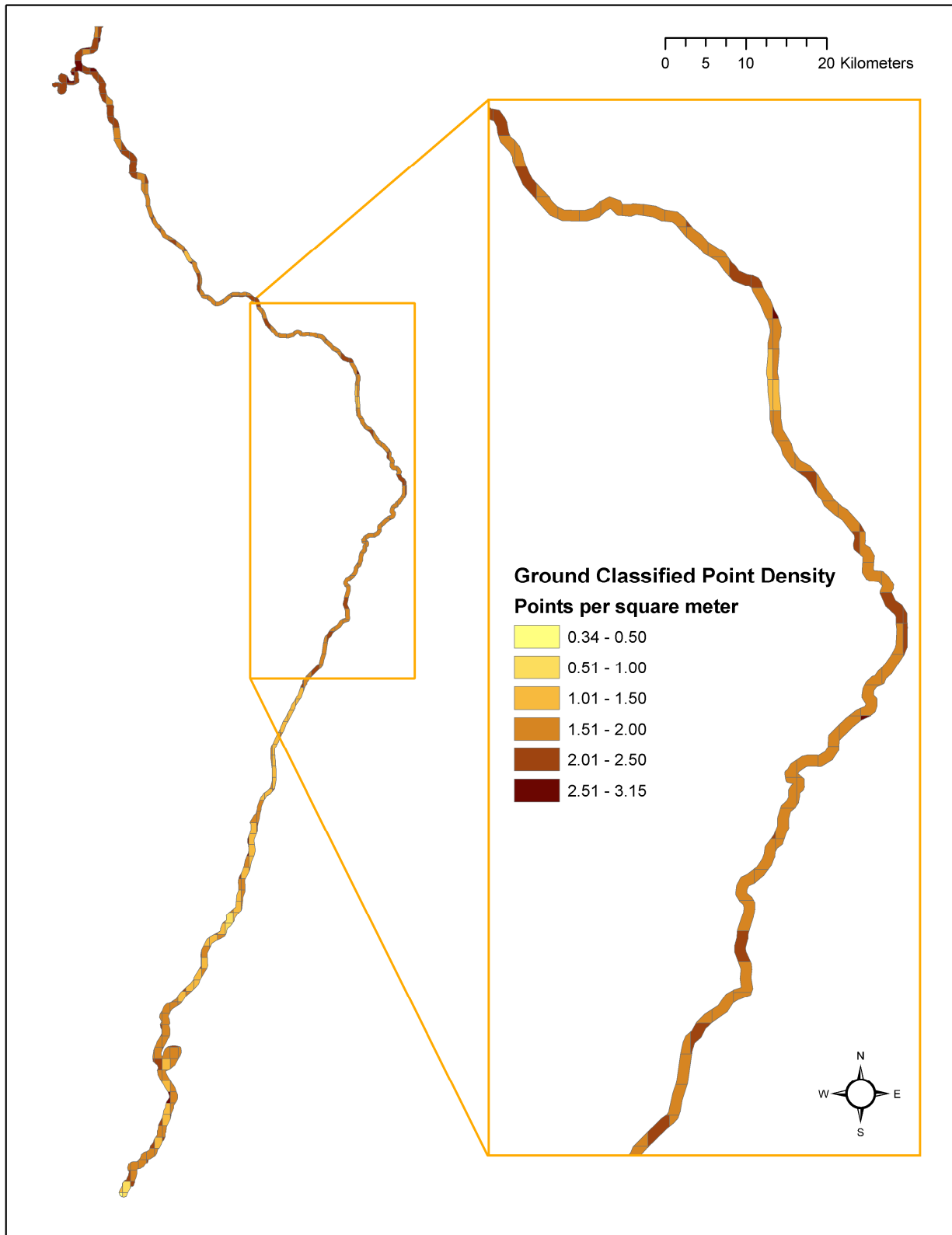


Figure 34. Delivery 12, UTM 11 density distribution map for ground classified points by USGS 0.75 minute quads.

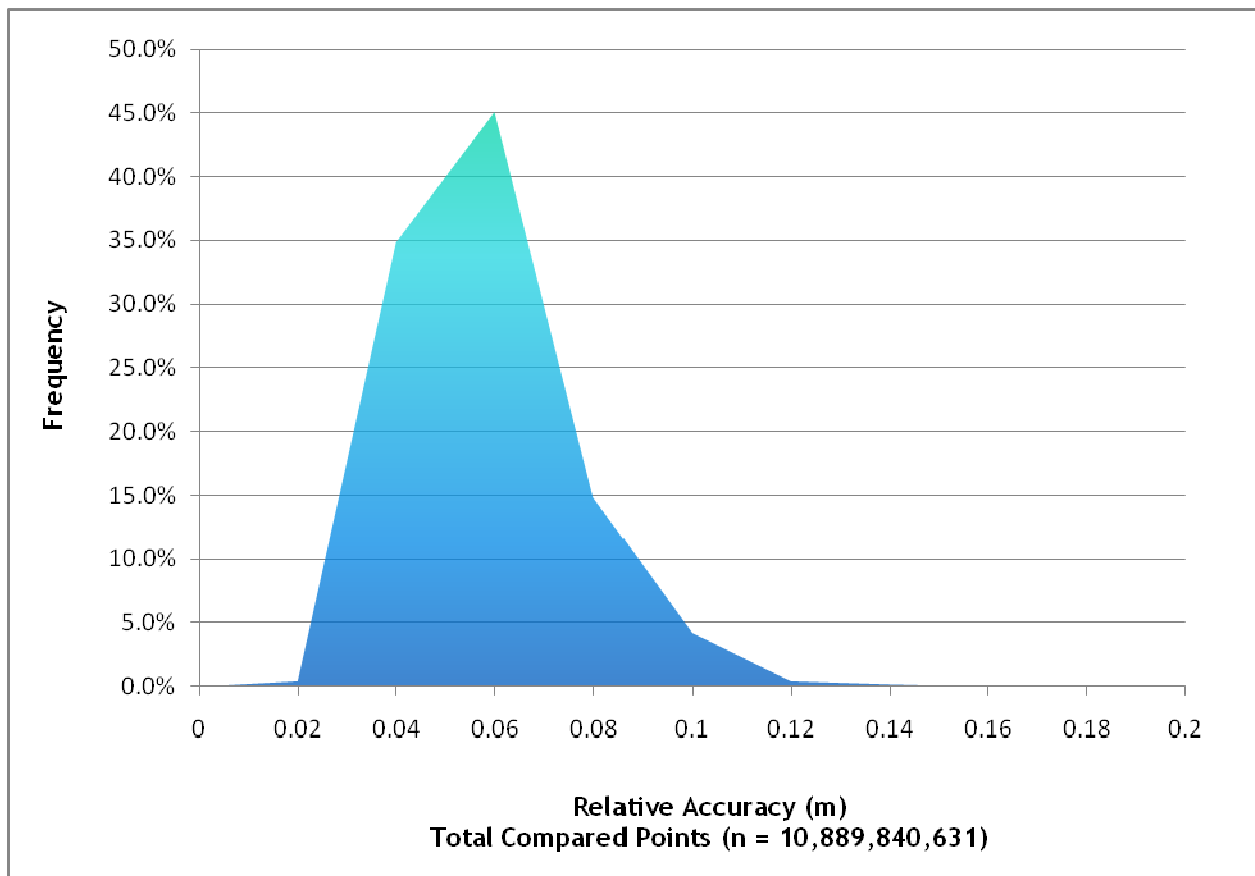


5.3 Relative Accuracy Calibration Results

Relative accuracy statistics for UTM 10

- Project Average = 0.042m
- Median Relative Accuracy = 0.045m
- 1σ Relative Accuracy = 0.016m
- 1.96σ Relative Accuracy = 0.032m

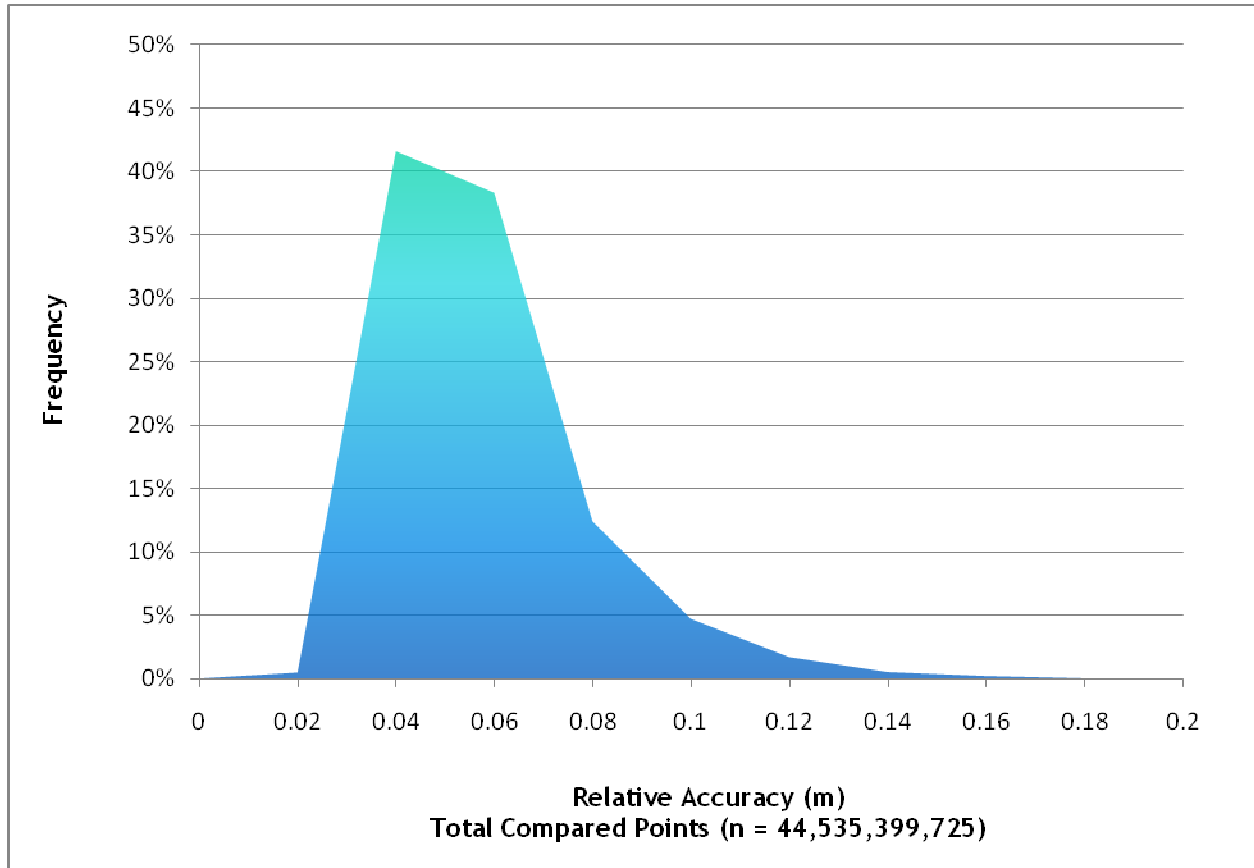
Figure 35. Distribution of relative accuracies per flight line, non slope-adjusted for UTM 10.



Relative accuracy statistics for UTM 11

- Project Average = 0.044m
- Median Relative Accuracy = 0.043m
- 1 σ Relative Accuracy = 0.020m
- 1.96 σ Relative Accuracy = 0.038m

Figure 36. Distribution of relative accuracies per flight line, non slope-adjusted for UTM 11.



5.4 Absolute Accuracy

Absolute accuracies for the Columbia River survey areas:

Table 5. Absolute Accuracy for UTM 10 - Deviation between laser points and RTK hard surface survey points.

RTK Survey Sample Size (n): 11,440		
Root Mean Square Error (RMSE) = 0.044m		Minimum Δz = -0.204m
Standard Deviations		Maximum Δz = 0.156m
1 sigma (σ): 0.044m	1.96 sigma (σ): 0.087m	Average Δz = -0.002m

Figure 37. Absolute Accuracy - Histogram Statistics, based on 11,440 RTK points in UTM 10.

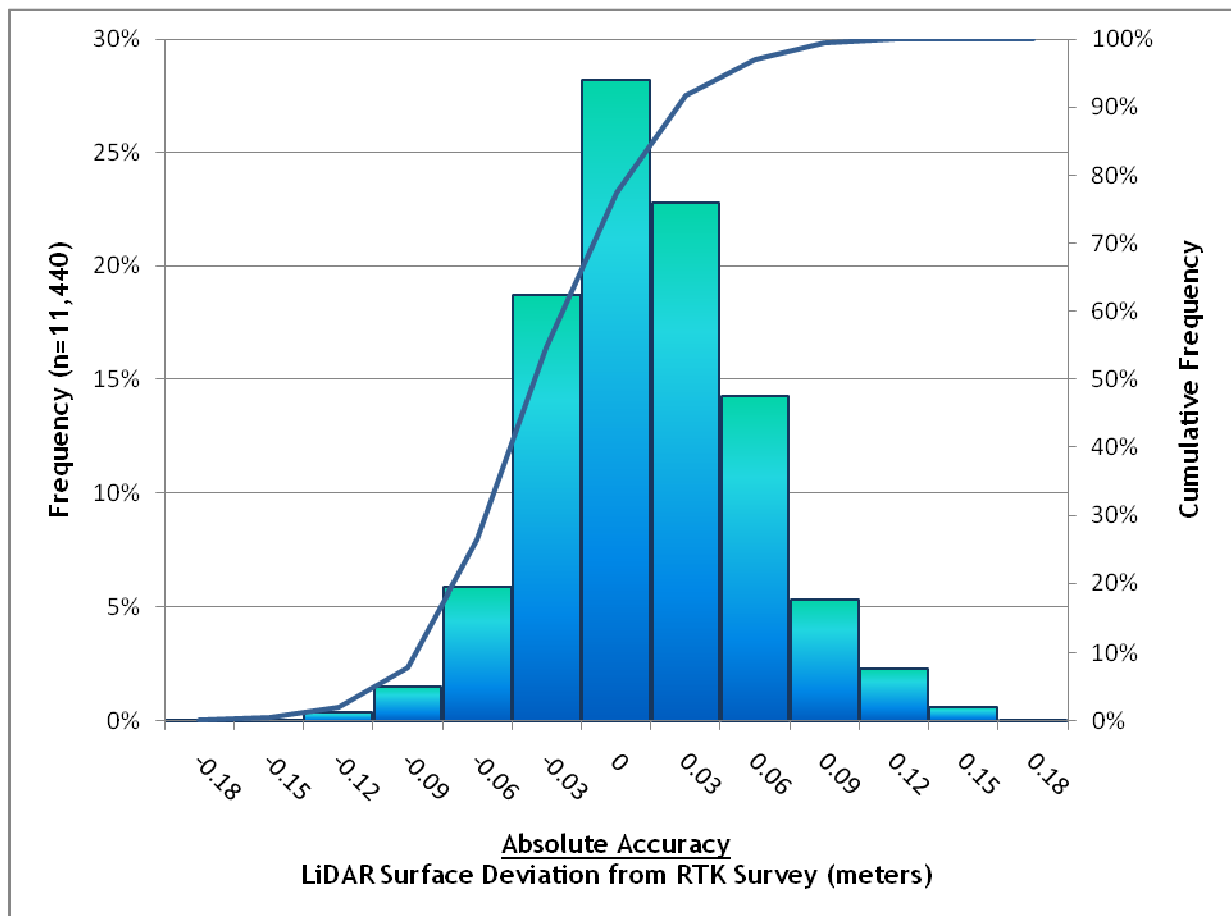
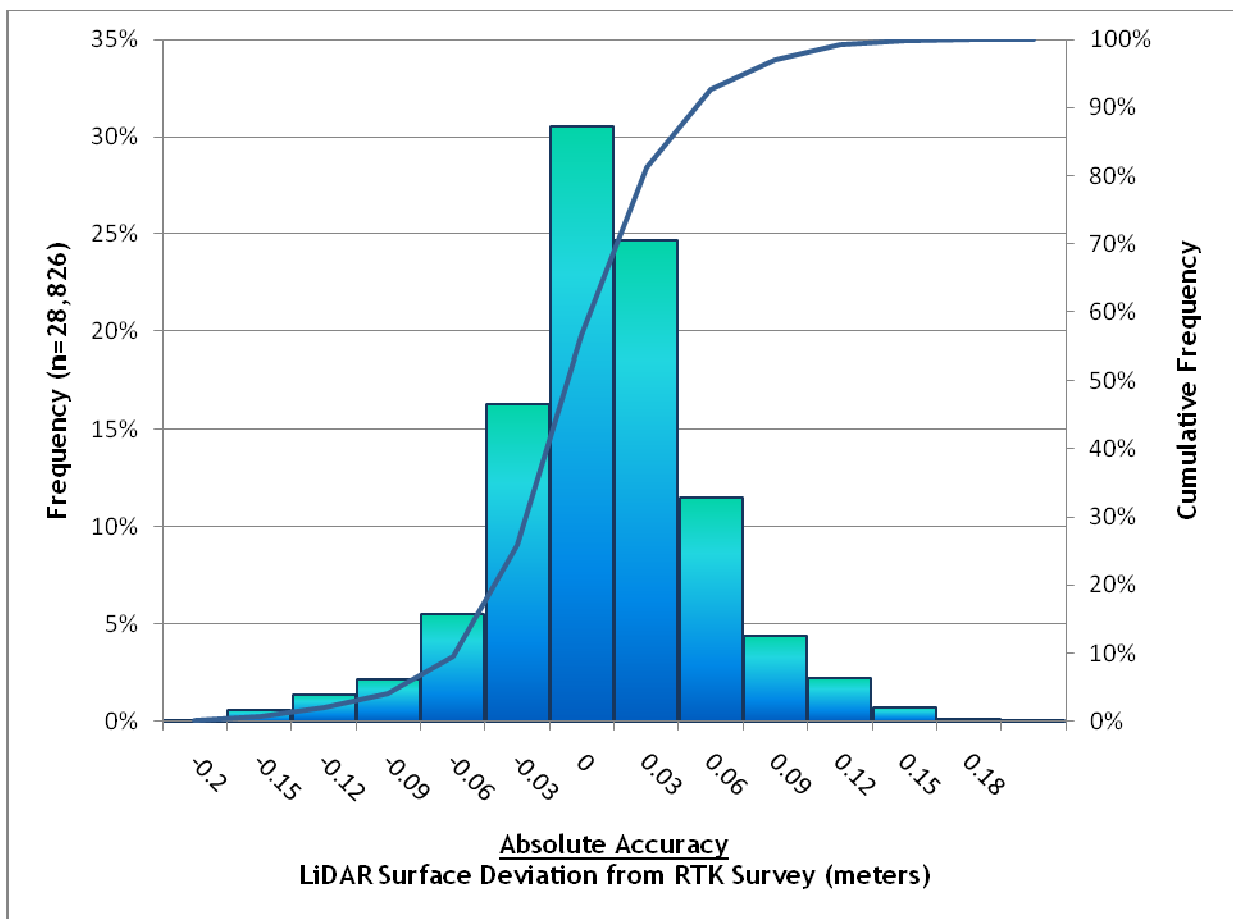


Table 6. Absolute Accuracy for UTM 11 - Deviation between laser points and RTK hard surface survey points.

RTK Survey Sample Size (n): 28,826	
Root Mean Square Error (RMSE) = 0.047m	Minimum Δz = -0.260m
Standard Deviations	Maximum Δz = 0.202m
1 sigma (σ): 0.047m 1.96 sigma (σ): 0.092m	Average Δz = -0.005m

Figure 38. Absolute Accuracy - Histogram Statistics, based on 28,826 RTK points in UTM 11.



6. Breakline Enforced Terrain Model

David C. Smith and Associates (DSA) created breaklines for the Columbia River study area using LiDAR-grammetry techniques. **Table 7** describes the type and definition of each breakline collected. The breaklines were used to supplement the LiDAR data in creation of a final ground model. Water boundaries were enforced using hard breaklines and water surfaces were flattened based on the elevation from the breaklines. The breakline boundaries were also used to assign any points with ground or model key point classification within the water delineated areas as a water class.

Table 7. Breaklines collected for the Columbia River study area, see Appendix B for feature definitions.

Feature	Implementation
Breakline	Hard Breakline
Breakline Obscured	Hard Breakline
Water Main	Hard Breakline
Water Island	Hard Breakline
Water Other	Hard Breakline
Buildings	Provided as Feature

7. Projection/Datum and Units

	Projection:	UTM Zone 10 and 11, NAD 83
Datum	Vertical:	NAVD88 Geoid09
	Horizontal:	NAD83
	Units:	meters

8. Deliverables

Point Data:	<ul style="list-style-type: none"> All Returns (LAS 1.2 format)
Vector Data:	<ul style="list-style-type: none"> Tile Index of LiDAR points (USGS 0.75 minute quads, shapefile) Tile Index of DEM rasters (USGS 7.5 minute quads, shapefile) 1-hz SBET files (shapefile) Breaklines (dxf format) <i>provided by DSA</i> Watermask (dxf format) <i>provided by DSA</i>
Raster Data:	<ul style="list-style-type: none"> Elevation models (1 m resolution) <ul style="list-style-type: none"> Breakline Enforced Bare Earth Model (ESRI GRID format) Highest Hit Model (ESRI GRID format) Intensity images (GeoTIFF format, 1 m resolution)
Data Report:	Full report containing introduction, methodology, and accuracy

9. Selected Images

Figure 39. 3D view looking west along Brushy Creek, the bare earth image is colored by elevation.

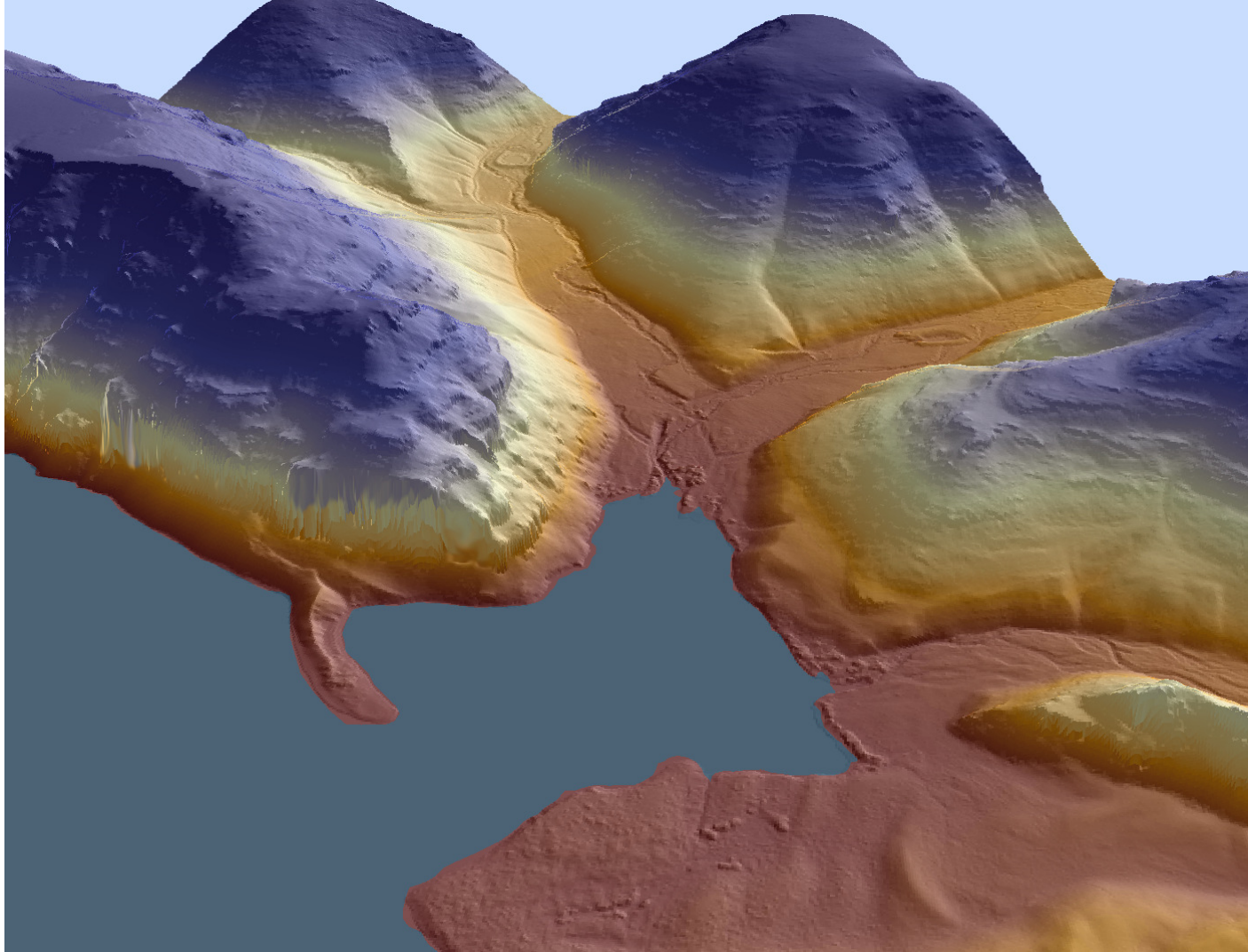


Figure 40. 3D point cloud looking north at I-5 crossing the Columbia River. MLK Blvd can be seen over I-5 and Portland Harbor is in the distance.

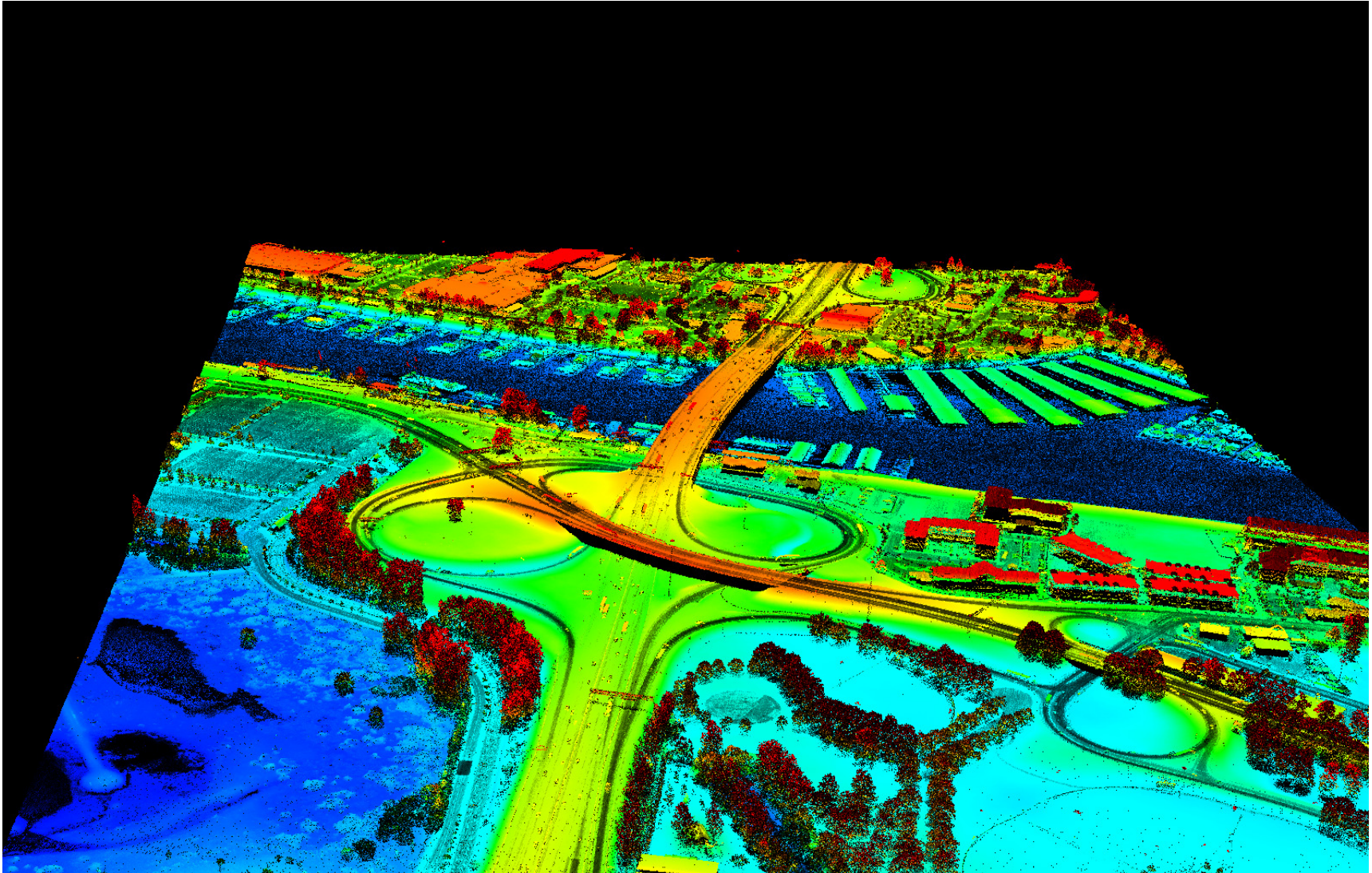


Figure 41. 3D point cloud looking southeast at middle section of Hayden island. A railroad bridge can be seen crossing the Columbia River with Portland Harbor in the far distant corner.

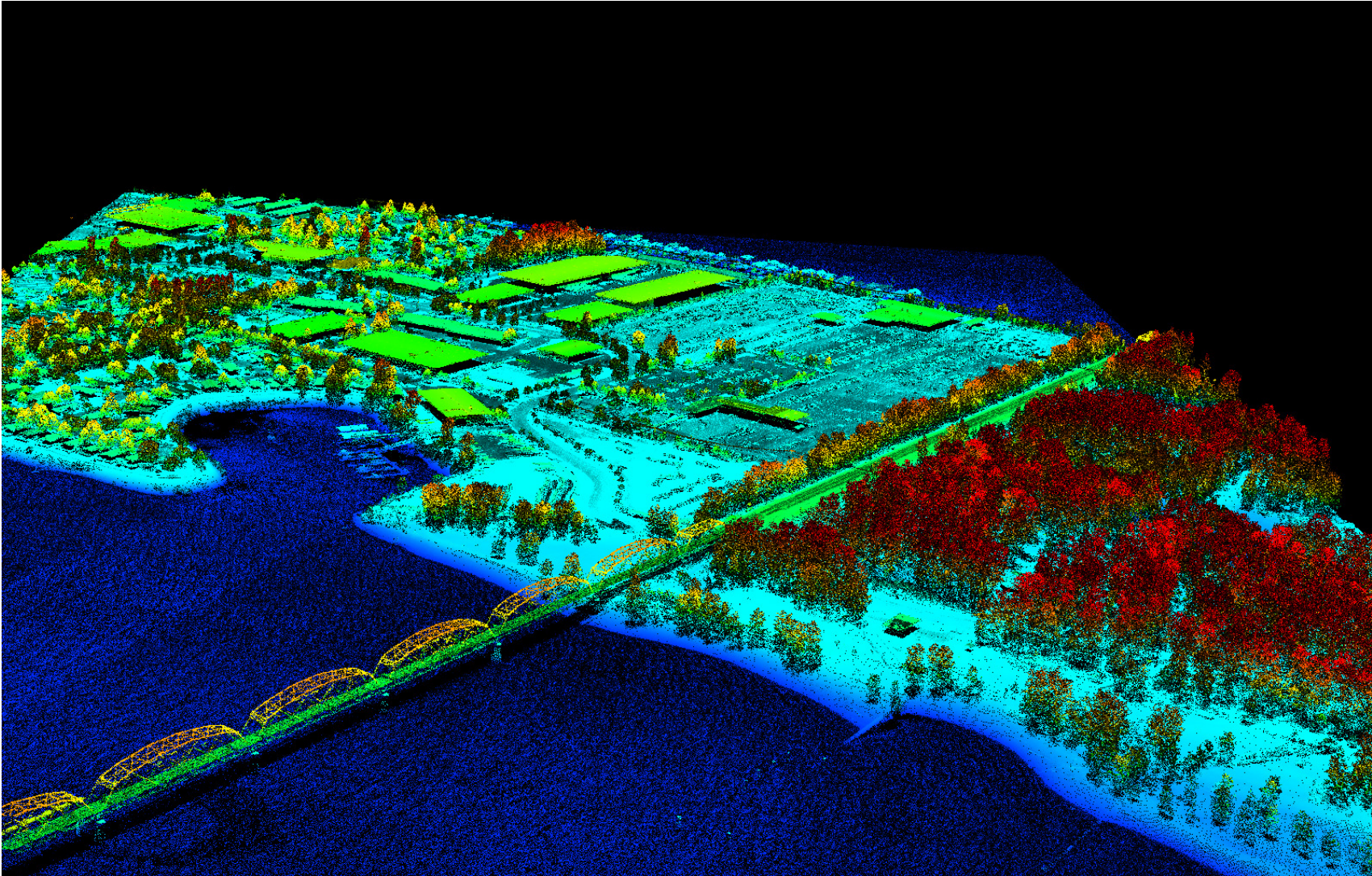


Figure 42. 3D view looking North along Longtain Creek. Top image is bare earth model colored by elevation, bottom image is NAIP draped over highest-hit model.

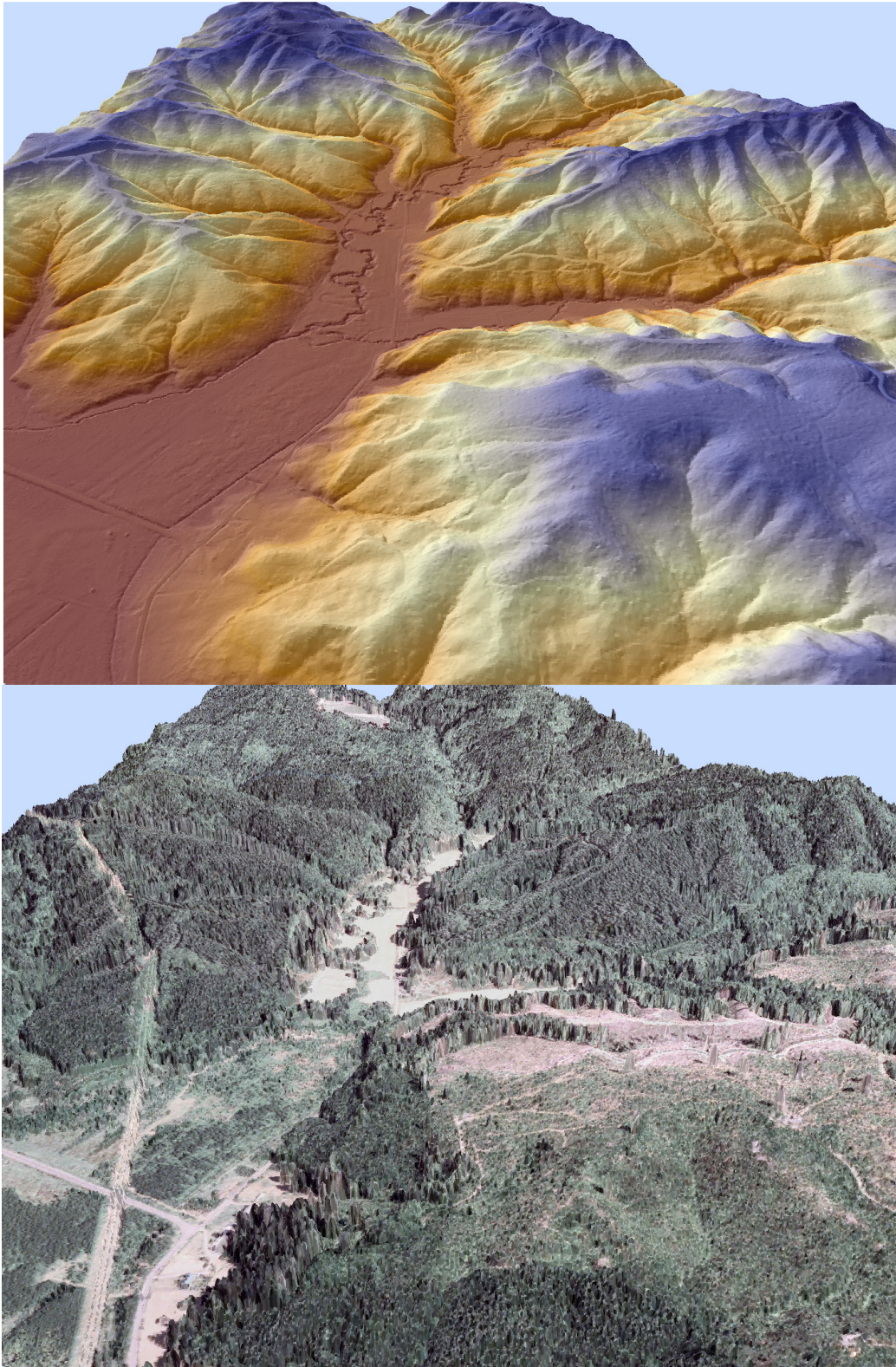


Figure 43. 3D view of West Longview looking North with Coal Creek Slough in the background. Top image is bare earth model colored by elevation, bottom image is NAIP draped over highest-hit model.



Figure 44. 3D view looking south along Franklin D Roosevelt Lake. Top image is bare earth model colored by elevation, bottom image is NAIP draped over highest-hit model.

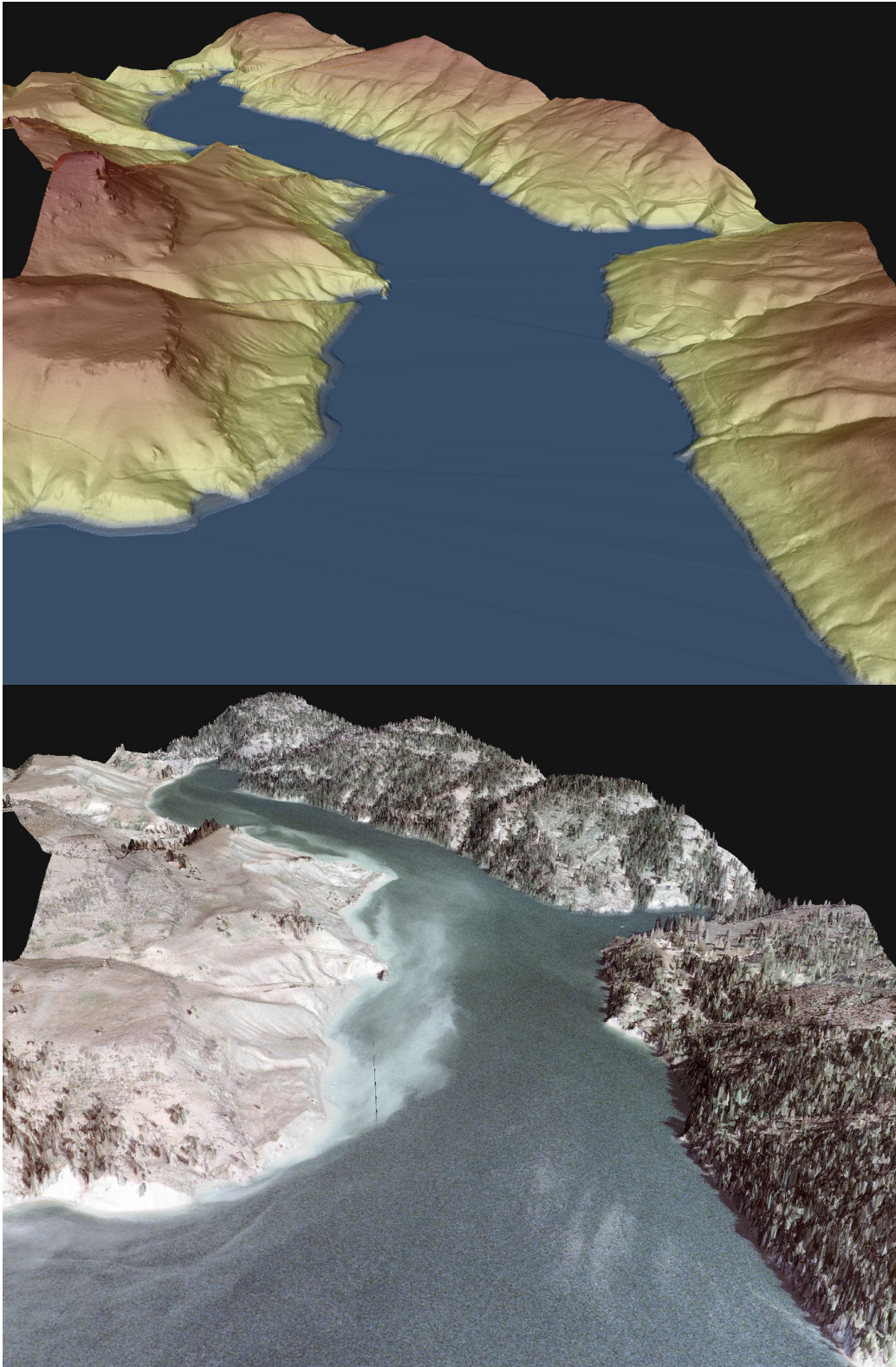


Figure 45. 3D view of Crescent Bay looking south. Top image is bare earth model colored by elevation, bottom image is NAIP draped over highest-hit model.

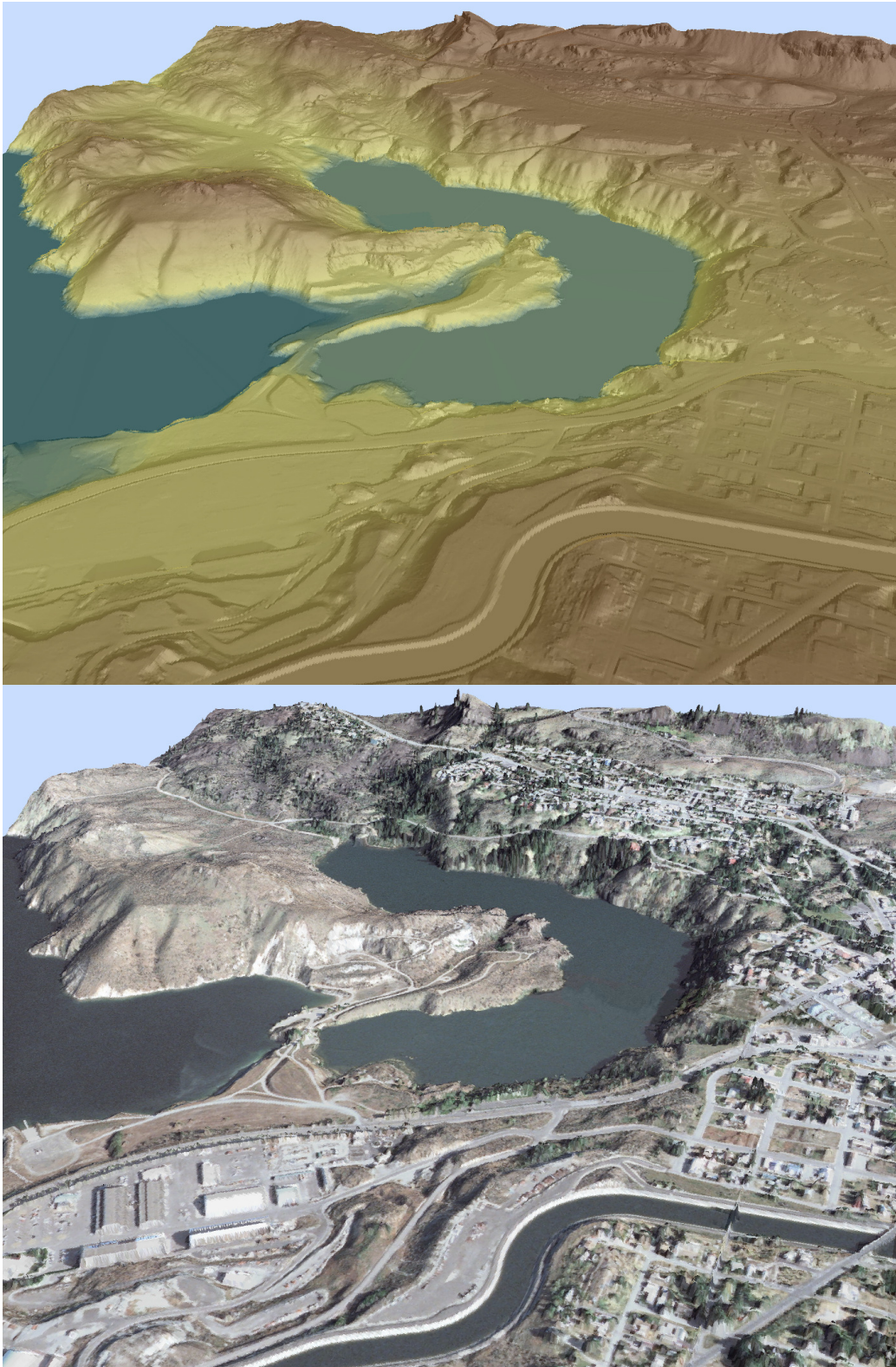


Figure 46. 3D view of Lewis and Clark Highway east of Cook, Washington along the Columbia River. Top image is bare earth model colored by elevation, bottom image is 2009 NAIP draped over highest-hit model.

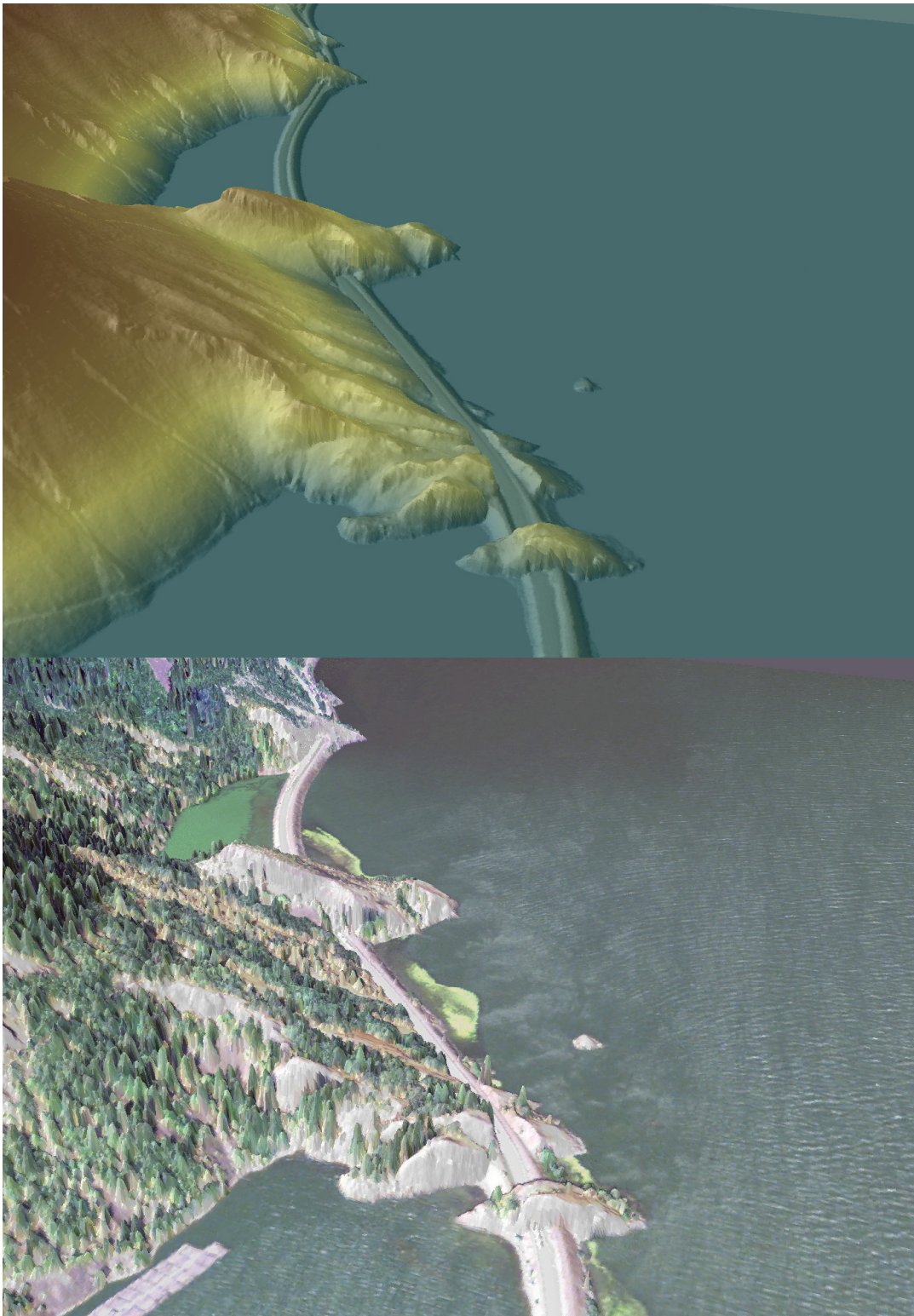


Figure 47. LiDAR point cloud colored by 2004 NAIP imagery. View looking north near Bonners Ferry, ID.



LiDAR Data Acquisition and Processing: Columbia River Survey, Final Delivery

Prepared by Watershed Sciences, Inc.

Figure 48. LiDAR point cloud colored by elevation. View looking Northwest from south of the Kootenai National Wildlife Refuge. A railroad track crosses through the scene.



Figure 49. LiDAR point cloud colored by elevation. View looking Southeast at Somers Marina in Somers, MT along Flathead Lake.

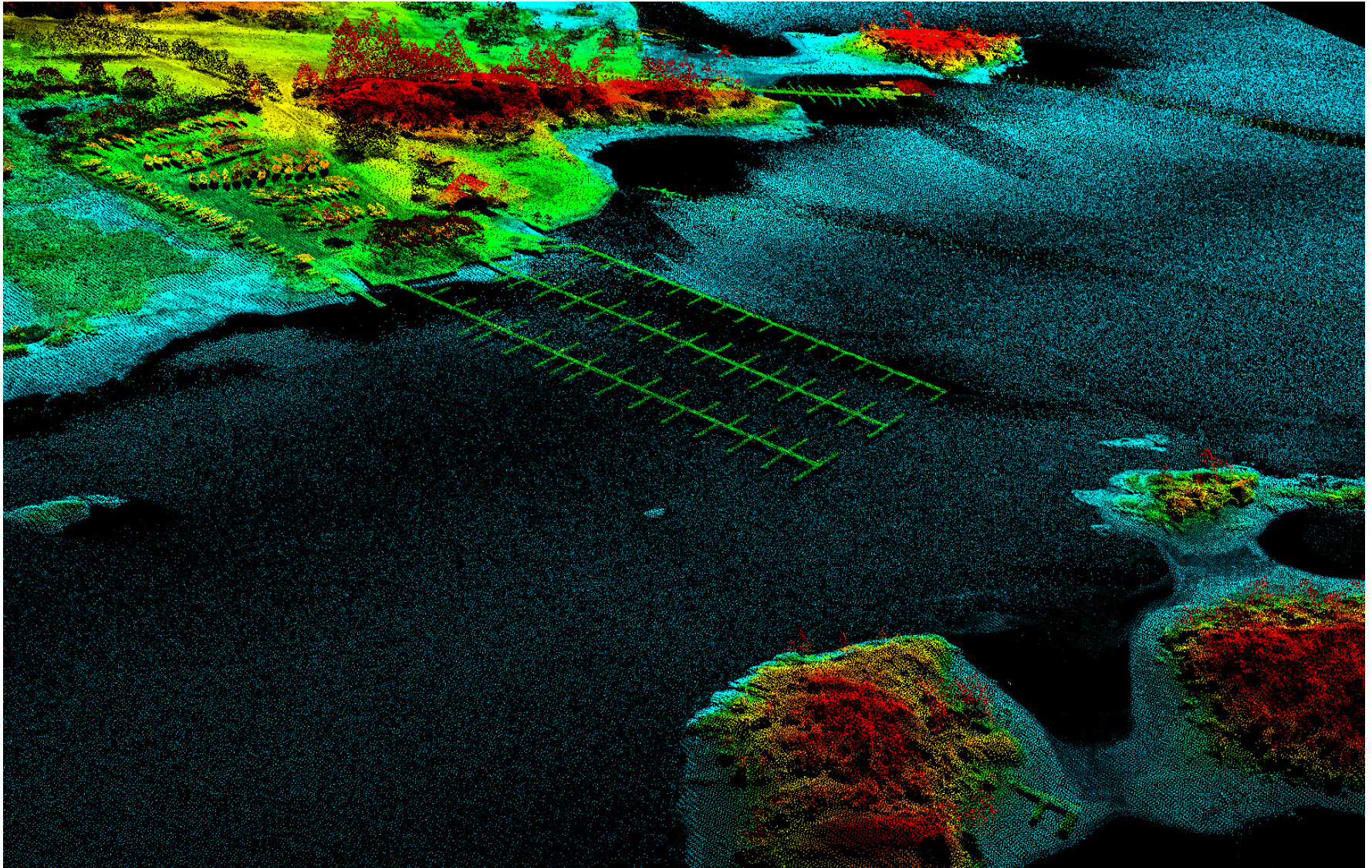


Figure 50. LiDAR point cloud colored by elevation. View looking East across Glacier Park International Airport.

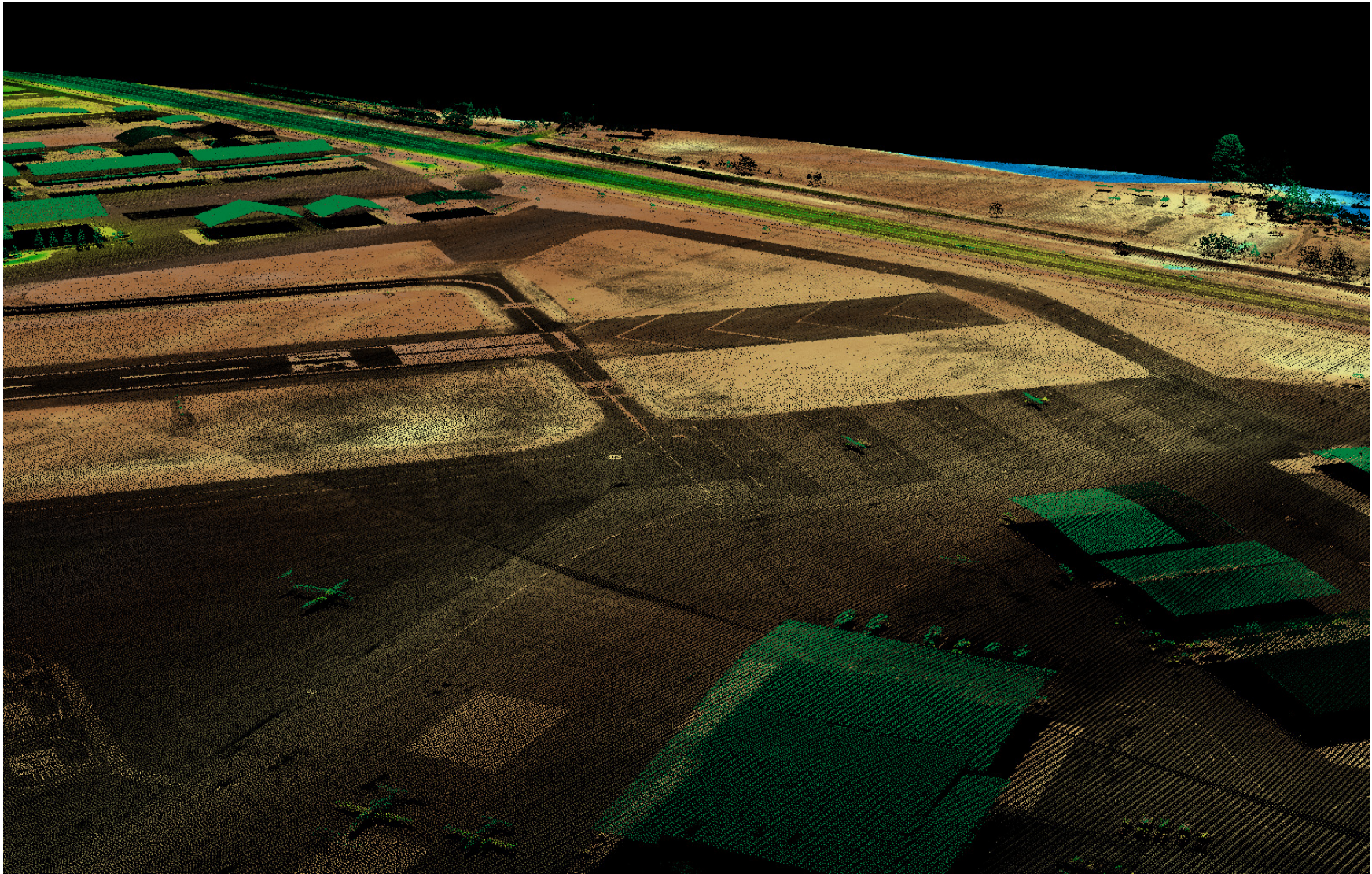


Figure 51. LiDAR point cloud colored by 2005 NAIP imagery. View looking southwest towards Oxbow Dam on the Snake River.



10. Glossary

1-sigma (σ) Absolute Deviation: Value for which the data are within one standard deviation (approximately 68th percentile) of a normally distributed data set.

2-sigma (σ) Absolute Deviation: Value for which the data are within two standard deviations (approximately 95th percentile) of a normally distributed data set.

Root Mean Square Error (RMSE): A statistic used to approximate the difference between real-world points and the LiDAR points. It is calculated by squaring all the values, then taking the average of the squares and taking the square root of the average.

Pulse Rate (PR): The rate at which laser pulses are emitted from the sensor; typically measured as thousands of pulses per second (kHz).

Pulse Returns: For every laser pulse emitted, the Leica ALS 50 Phase II system can record *up to four* wave forms reflected back to the sensor. Portions of the wave form that return earliest are the highest element in multi-tiered surfaces such as vegetation. Portions of the wave form that return last are the lowest element in multi-tiered surfaces.

Accuracy: The statistical comparison between known (surveyed) points and laser points. Typically measured as the standard deviation (σ) and root mean square error (RMSE).

Intensity Values: The peak power ratio of the laser return to the emitted laser. It is a function of surface reflectivity.

Data Density: A common measure of LiDAR resolution, measured as points per square meter.

Spot Spacing: Also a measure of LiDAR resolution, measured as the average distance between laser points.

Nadir: A single point or locus of points on the surface of the earth directly below a sensor as it progresses along its flight line.

Scan Angle: The angle from nadir to the edge of the scan, measured in degrees. Laser point accuracy typically decreases as scan angles increase.

Overlap: The area shared between flight lines, typically measured in percents; 100% overlap is essential to ensure complete coverage and reduce laser shadows.

DTM / DEM: These often-interchanged terms refer to models made from laser points. The digital elevation model (DEM) refers to all surfaces, including bare ground and vegetation, while the digital terrain model (DTM) refers only to those points classified as ground.

Real-Time Kinematic (RTK) Survey: GPS surveying is conducted with a GPS base station deployed over a known monument with a radio connection to a GPS rover. Both the base station and rover receive differential GPS data and the baseline correction is solved between the two. This type of ground survey is accurate to 1.5 cm or less.

11. Citations

David Evans and Associates, Inc. 2010. Columbia River Treaty: OPUS DB Data Sheets. DVD. Solicitation No. W9127N-09-D-0009.

Soininen, A. 2004. TerraScan User's Guide. TerraSolid.

Appendix A

LiDAR accuracy error sources and solutions:

Type of Error	Source	Post Processing Solution
GPS (Static/Kinematic)	Long Base Lines	None
	Poor Satellite Constellation	None
	Poor Antenna Visibility	Reduce Visibility Mask
Relative Accuracy	Poor System Calibration	Recalibrate IMU and sensor offsets/settings
	Inaccurate System	None
Laser Noise	Poor Laser Timing	None
	Poor Laser Reception	None
	Poor Laser Power	None
	Irregular Laser Shape	None

Operational measures taken to improve relative accuracy:

1. Low Flight Altitude: Terrain following is employed to maintain a constant above ground level (AGL). Laser horizontal errors are a function of flight altitude above ground (i.e., ~ 1/3000th AGL flight altitude).
2. Focus Laser Power at narrow beam footprint: A laser return must be received by the system above a power threshold to accurately record a measurement. The strength of the laser return is a function of laser emission power, laser footprint, flight altitude and the reflectivity of the target. While surface reflectivity cannot be controlled, laser power can be increased and low flight altitudes can be maintained.
3. Reduced Scan Angle: Edge-of-scan data can become inaccurate. The scan angle was reduced to a maximum of $\pm 15^\circ$ from nadir, creating a narrow swath width and greatly reducing laser shadows from trees and buildings.
4. Quality GPS: Flights took place during optimal GPS conditions (e.g., 6 or more satellites and PDOP [Position Dilution of Precision] less than 3.0). Before each flight, the PDOP was determined for the survey day. During all flight times, a dual frequency DGPS base station recording at 1-second epochs was utilized and a maximum baseline length between the aircraft and the control points was less than 19 km (11.5 miles) at all times.
5. Ground Survey: Ground survey point accuracy (i.e. <1.5 cm RMSE) occurs during optimal PDOP ranges and targets a minimal baseline distance of 4 miles between GPS rover and base. Robust statistics are, in part, a function of sample size (n) and distribution. Ground survey RTK points are distributed to the extent possible throughout multiple flight lines and across the survey area.
6. 50% Side-Lap (100% Overlap): Overlapping areas are optimized for relative accuracy testing. Laser shadowing is minimized to help increase target acquisition from multiple scan angles. Ideally, with a 50% side-lap, the most nadir portion of one flight line coincides with the edge (least nadir) portion of overlapping flight lines. A minimum of 50% side-lap with terrain-followed acquisition prevents data gaps.
7. Opposing Flight Lines: All overlapping flight lines are opposing. Pitch, roll and heading errors are amplified by a factor of two relative to the adjacent flight line(s), making misalignments easier to detect and resolve.

QA/QC Data issue responses:

An area within tile 48116F2206 was identified by DSA as a data issue. Watershed Sciences, Inc. has reviewed the LiDAR point data at this site and noted a high bridge and a steep slope. LiDAR acquisition in areas of steep terrain can create shadowing that result in low point density. Recorded flightline data indicates that acquisition was conducted according to contract specifications in this area. The lack of ground classified points represents a limitation of current LiDAR technology. However, the use of water's edge and terrain breaklines in conjunction with the LiDAR has allowed the model to interpolate through the dataset.

Figure 52. Overhead view and cross section of LiDAR point data issue in tile 48116F2206 (Kootenai River)

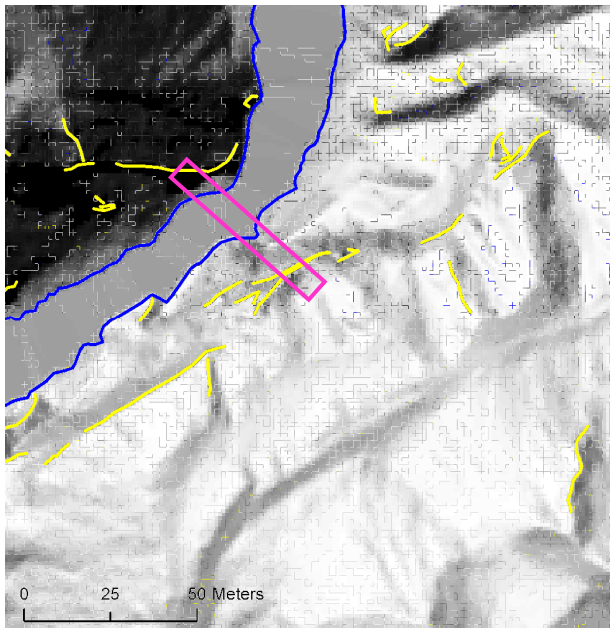
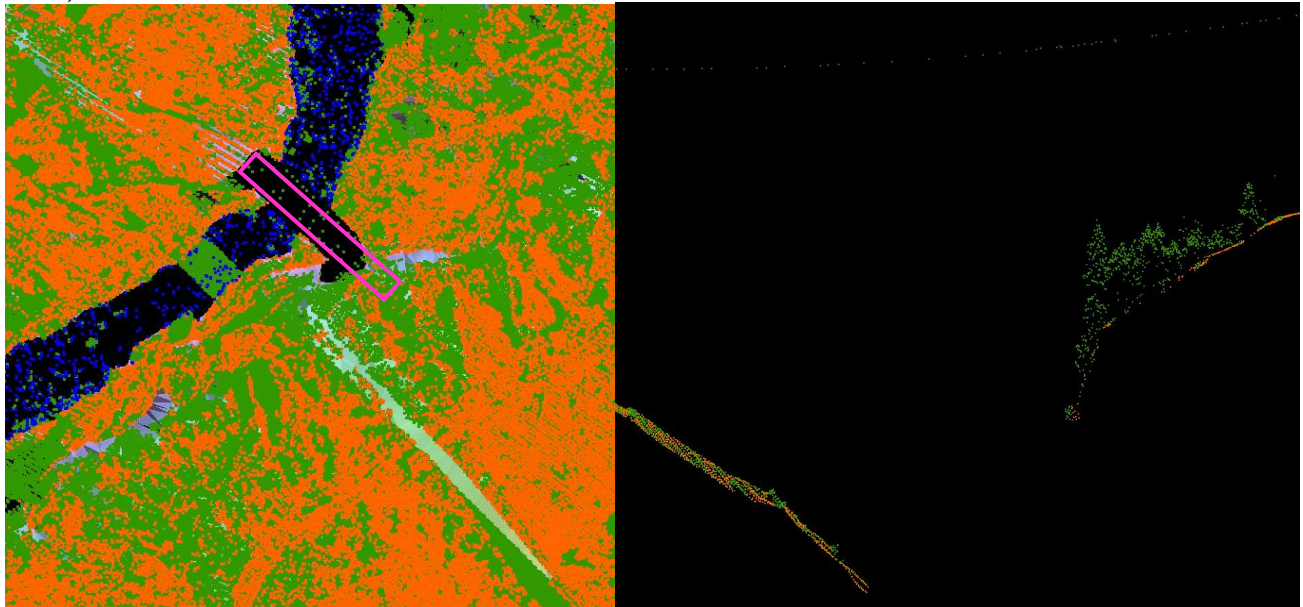


Figure 53. Resulting bare earth model with breaklines applied. Yellow lines are terrain breaks and blue lines are water breaklines.

Appendix B

Breakline definitions as determined by DSA:

FEATURE:

BREAKLINE - Added to the ground model where the LiDAR ground points were missing or not properly defining the surface. Usually occurred on sharp breaks associated with cliffs. These breaks are derived from the 1st return data and fit to the ground data.

BREAKLINE_OBSCURE - Added in vegetated areas where the LiDAR ground model was not complete due to dense vegetation. These lines are interpreted from visible data and fit to visible ground data.

WATER_MAIN - Main rivers, not including side rivers and streams. Designed to be the river in the center of the coverage area, Columbia, Snake, etc.

WATER_OTHER - Covers side rivers, lakes, ponds etc. This coverage is not intended to capture all water outside the main rivers but only water edges that need a breakline and need LiDAR data re-classified. No single line streams are collected.

WATER_ISLAND - Islands in the rivers and streams.

BUILDING - Visible and obvious buildings.

BUILDING_UNSURE - Features that appear to be buildings but might not be.

BUILDING_AREA - Large areas with a dense population of buildings, subdivisions, etc.